Journal of Medicinal Chemistry

Article

pubs.acs.org/jmc

Optimization and Structure–Activity Relationships of Phosphinic Pseudotripeptide Inhibitors of Aminopeptidases That Generate Antigenic Peptides

Paraskevi Kokkala,[†] Anastasia Mpakali,[‡] Francois-Xavier Mauvais,[§] Athanasios Papakyriakou,[‡] Ira Daskalaki,[†] Ioanna Petropoulou,[†] Sofia Kavvalou,[†] Mirto Papathanasopoulou,[†] Stefanos Agrotis,[†] Theodora-Markisia Fonsou,[†] Peter van Endert,[§] Efstratios Stratikos,*[,‡] and Dimitris Georgiadis*[,†]

[†]Laboratory of Organic Chemistry, Department of Chemistry, National and Kapodistrian University of Athens, Panepistimiopolis, Zografou, 15771, Athens, Greece

[‡]National Center for Scientific Research "Demokritos", GR 15310 Agia Paraskevi, Attikis, Greece

[§]Institut National de la Santé et de la Recherche Médicale, Unité 1151, Université Paris Descartes, Sorbonne Paris Cité, Centre National de la Recherche Scientifique, Unité 8253, 75015 Paris, France

Supporting Information

ABSTRACT: The oxytocinase subfamily of M1 aminopeptidases, consisting of ER aminopeptidase 1 (ERAP1), ER aminopeptidase 2 (ERAP2), and insulin-regulated aminopeptidase (IRAP), plays critical roles in the generation of antigenic peptides and indirectly regulates human adaptive immune responses. We have previously demonstrated that phosphinic pseudotripeptides can constitute potent inhibitors of this group of enzymes. In this study, we used synthetic methodologies able to furnish a series of stereochemically defined phosphinic pseudotripeptides and demonstrate that side chains at P_1' and P_2' positions are critical determinants in driving potency and selectivity. We identified low nanomolar inhibitors of ERAP2 and IRAP that display selectivity of more than 2 and 3 orders of magnitude, respectively. Cellular analysis demonstrated that one of the compounds that is a selective IRAP inhibitor can reduce IRAP-dependent but not ERAP1-dependent cross-presentation by dendritic cells with nanomolar efficacy. Our results encourage further preclinical development of phosphinic pseudotripeptides as regulators of adaptive immune responses.

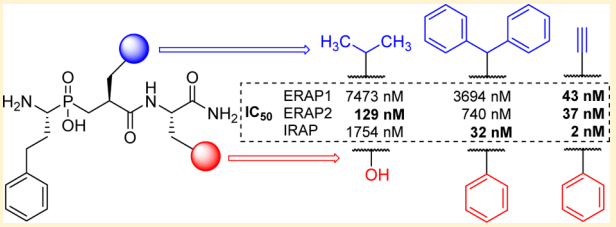

INTRODUCTION

Antigen processing aminopeptidases (APAs) trim antigenic peptide precursors and generate peptides for binding onto major histocompatibility complex class I (MHCI) molecules.[1] The peptide–MHCI complex is then transported to the cell surface of somatic cells and presented to circulating T lymphocytes. Interactions between specialized T-cell receptors and peptide–MHCI complexes are used to determine if the cell is infected or otherwise aberrant, initiating biochemical cascades that lead to apoptosis.[2] Three major APAs have been identified to date: ER aminopeptidase 1 (ERAP1), ER aminopeptidase 2 (ERAP2), and insulin-regulated aminopeptidase (IRAP).[3] The first two are localized in the ER and trim antigenic peptide precursors translocated into the ER but generated in the cytosol.[2] IRAP trims antigenic peptide precursor generated by endocytosed proteins in dendritic cells for cross-presentation.[4] These three enzymes are highly homologous (50% sequence identity on average) and have conserved active sites, although key amino acid differences defining the specificity pockets can account for different substrate preferences.[5] Structural differences between the three enzymes also include a unique orientation of the GAMEN motif in IRAP[5b] and an overall conformational change that reorganizes the structure from an open to a closed form, affecting the folding of the active site and nearby specificity pockets.[6]

The enzymatic activity and expression level of APAs, frequently affected by polymorphic variation, has been repeatedly associated with predisposition to autoimmunity, infections, and cancer immune evasion.[7] Functional studies have established that alterations in the enzymatic activity of APAs can result in changes in the presented antigenic peptides and concomitant cytotoxic responses by T-cells.[8] Furthermore, the activity of ERAP1 has been also linked to the function of innate immune responses.[9] Accumulating evidence has therefore established the tractability of these enzymes as pharmaceutical targets for the regulation of immune responses.[10]

We have previously demonstrated that a phosphinic pseudotripeptide, **6e** (DG013A), can act as a highly potent inhibitor of all three APAs and is able to regulate antigen presentation in cellular systems (Figure 1).[11] This nanomolar

Received: July 12, 2016

DOI: 10.1021/acs.jmedchem.6b01031
J. Med. Chem. XXXX, XXX, XXX–XXX

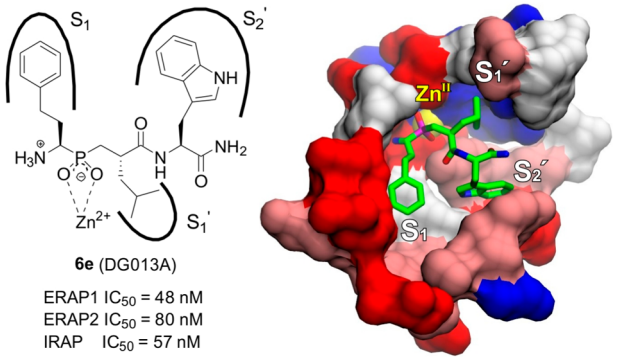

Figure 1. Structure, in vitro inhibition data, and schematic representation of **6e** in the active site of ERAP2 (PDB code 4JBS), illustrating the three interacting subsites that are color-coded per residue type (white, nonpolar; pink, polar; red, acidic; blue, basic). The inhibitor is shown as sticks with green C, blue N, red O, magenta P, and the catalytic Zn(II) as a yellow sphere.

potency inhibitor was shown to be able to enhance anticancer cytotoxic responses and to down-regulate T-cell mediated and innate inflammatory responses, indicating that this class of compounds holds promise for pharmaceutical applications.[11,12] Low selectivity between the three APAs, however, limits options for preclinical development. However, since this inhibitor utilizes the three first specificity pockets of these aminopeptidases, as it was revealed by X-ray crystallographic analysis of **6e**/ERAP2 complex (Figure 1),[11] varying the side chains that occupy these pockets can be a valid approach for optimizing both selectivity and potency. The ability of phosphinic pseudopeptides to successfully discriminate active sites with high structural homology and functional similarity has been well-demonstrated in several demanding cases in the past, such as the development of domain-selective inhibitors of angiotensin-converting enzyme[13] and a selective subnanomolar inhibitor of MMP-12.[14] This property of phosphinic peptides, as compared to other classes of protease inhibitors, is attributed to the weak zinc-binding ability of phosphinic group which allows for inhibitor affinity to be determined by proper optimization of weaker but more specific enzyme−ligand interactions and not by the dominance of tight chelating interactions with the zinc ion.[15]

In this study, we focused on the structure−activity relationships (SAR) of P_1' and P_2' side chains in driving potency and selectivity for APAs, by synthesizing a series of stereochemically defined phosphinic pseudotripeptide derivatives. In vitro evaluation and molecular modeling revealed that while aromatic residues at P_2' position are critical for achieving potency for ERAP1, hydrophilic residues at the same site can enhance selectivity for ERAP2. Conversely, although small P_1' side chains are important for achieving potency, bulkier groups can be well tolerated only by IRAP resulting in selective inhibitors. We identified several new nanomolar-affinity selective inhibitors for ERAP2 and IRAP that displayed selectivity for each enzyme of over 2 and 3 orders of magnitude, respectively. Proof-of-concept cellular analysis using a cross-presentation model system indicated that one of the selective IRAP inhibitors can reduce IRAP-dependent but not ERAP1-dependent cross-presentation by dendritic cells with nanomolar efficacy. Our results encourage further preclinical development of phosphinic pseudotripeptides for therapeutic applications.

RESULTS AND DISCUSSION

Inhibitor Design. In previous studies, it has been demonstrated that **6e** influences with high efficacy antigen presentation in several cell-based systems. For this reason, we were based on the core structure of **6e** and used it as a template for screening various modifications at P_1' and P_2' positions, aiming to enhance potency and selectivity. The factor of stereochemical purity was set as a priority, even though available synthetic possibilities to achieve this goal are extremely limited.[16] This requirement can be critical for the accurate evaluation of structure−activity relationships and the discovery of improved inhibitors, especially in terms of selectivity. Interestingly, inversion of the selectivity exhibited by different diastereoisomers has been recently highlighted in the case of phosphinic tripeptide inhibitors of neprilysin (NEP) and endothelin-converting enzyme (ECE-1).[17] In a noteworthy example from this report, the 20-fold selectivity for NEP achieved by using a mixture of P_1'-epimers of a phosphinic tripeptide dropped down to a 5-fold selectivity for NEP when the "natural" P_1'-epimer was employed, and this was inversed to a 500-fold selectivity for ECE-1 when the "unnatural" P_1'-epimer was examined. Notably, most of the studies related to phosphinic peptide inhibitors of Zn aminopeptidases involve evaluation of diastereoisomeric mixtures,[18] with only a few exceptions.[19] To our knowledge, in the only relevant systematic study a large selection of stereochemically pure phosphinic tripeptides was evaluated but all of them were isolated after separation by RP-HPLC of the final diastereoisomeric mixtures of inhibitors.[19a] In our case, considering the 2−3 orders of magnitude difference in affinity between two different diastereoisomers of **6e** (epimers at P_1' position, **6e** and **6e′**)[11] and with the aim to eliminate possible inaccuracies during SAR analysis, we devised appropriately adjusted synthetic plans to control the stereochemical purity and identity of final compounds. Most of the inhibitors presented herein were obtained as single diastereoisomers directly from the synthesis, using late-stage diversification approaches on stereochemically pure building blocks. In order to explore the S_1' cavity of target aminopeptidases, we based our synthesis on a well-studied postmodification protocol of phosphinic peptides, which has been developed several years ago in our laboratory.[20] This strategy affords diverse, linear isoxazole-substituted P_1' side chains and has been successfully applied in the past to the discovery of inhibitors for other families of Zn metalloproteases[14,17a,21] but not for aminopeptidases. Finally, nonlinear P_1' substitutions were pursued in order to estimate the effect of expanding the bulk of side chains toward more than one direction. This differentiation in the spatial installation of bulky groups at P_1' position revealed significant variations between inhibitors with linear "extended" and nonlinear "expanded" P_1' side chains, as it will be discussed below.

Chemistry. For the synthesis of compounds **6a−k**, our efforts were focused on the preparation of parent phosphinic building block **4** in a stereochemically pure form (Scheme 1). Stereochemical purity was considered essential during our design in order to extract accurate structure−activity relationships that would eventually reveal the structural determinants responsible for high potency and selectivity. Given the lack of general synthetic methods able to provide stereochemical control during the formation of P_1' stereogenic center of phosphinic peptides,[15] we explored the possibility of resolving diastereoisomeric mixtures by selective crystallization, a

DOI: 10.1021/acs.jmedchem.6b01031
J. Med. Chem. XXXX, XXX, XXX−XXX

Scheme 1. Synthesis of Phosphinic Building Block 4[a]

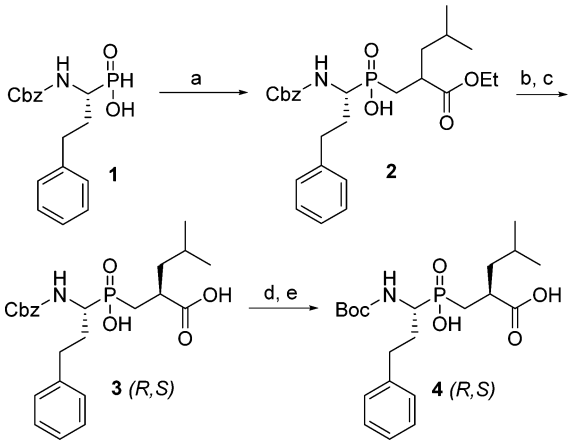

[a]Reagents and conditions: (a) HMDS, $H_2C{=}C[CH_2CH(CH_3)_2]$-COOEt, 110 °C, 1 h, then 90 °C, 3 h, then EtOH, 70 °C, 30 min; (b) NaOH, EtOH, H_2O, rt, 24 h, then H_3O^+; (c) 2× recrystallizations by AcOEt, 46%, three steps; (d) HBr/AcOH 33%, rt, 1 h; (e) Boc_2O, Et_3N, DMF, rt, 24 h, 92%, two steps.

technique that has previously succeeded in several cases of phosphinic dipeptide and tripeptide isosters.[17a,20,22] In this regard, the preparation of enantiomerically pure amino-phosphinic acid **1** by a scalable method was an absolute requirement for accomplishing our goal. It has been previously described in the literature that optically pure **1** can be obtained by HPLC enantiomeric separation of the corresponding racemic mixture;[23] however this approach is limited to milligram quantities.[19b] In contrast with earlier reports,[19b] we were pleased to find that resolution of diastereoisomeric salts of racemic **1** with (*S*)-(−)-α-methylbenzylamine by crystallization, following the protocol of Baylis et al., was highly efficient.[24] By this procedure, the levorotatory (*R*)-isomer (**1**)[23] [salt with (*S*)-(−)-amine, $[\alpha]_D^{20}$ −22.3 (*c* 1, EtOH); free acid, $[\alpha]_D^{20}$ −35.7 (*c* 1, EtOH)] was successfully isolated in a multigram quantities. P-Michael addition of **1** to ethyl 4-methyl-2-methylenepentanoate[25] using silylating conditions afforded **2** as a mixture of two diastereoisomers in nearly equimolar ratio (Scheme 1). All attempts of diastereoisomeric separation by crystallization at this stage failed; therefore compound **2** was subjected to saponification and crystallization efforts were repeated at racemic diacid **3**. Two recrystallizations by ethyl acetate proved sufficient for the gram-scale isolation of the less soluble **3** (*R,S*) isomer with dr > 95%, as determined by ^{31}P NMR. Finally, the Cbz group was exchanged by Boc following a two-step procedure. This exchange was considered necessary due to the advantageous behavior of Boc group during the final deprotection of target tripeptides, as compared to the Cbz group.

With the stereochemically pure building block **4** in hand, the synthesis of inhibitors **6a−k** required a coupling protocol that does not involve prior protection of the hydroxyphosphinyl moiety. In this regard, we employed a previously described, epimerization-free protocol based on the EDC/HOBt coupling system (Scheme 2).[20,22a] During optimization, high concentrations (0.5 mmol of substrate/1 mL of solvent) were found to be essential for efficient coupling reactions. Aiming to reach the final tripeptides **6a−k** in a single deprotection step, amino acid carboxamides **5a−k** with acid-labile protecting groups (if necessary) were employed (see Supporting Information for

Scheme 2. Synthesis of P_2' Diversified Phosphinic Pseudotripeptide Inhibitors 6a−k[a]

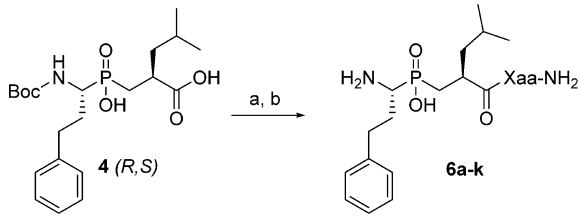

[a]Reagents and conditions: (a) H-Xaa-NH_2 (**5a−k**), [Xaa for **5a**: L-Ala. **5b**: L-Leu. **5c**: L-Phe. **5d**: L-Pro. **5e**: L-Trp. **5f**: L-Tyr(*t*-Bu). **5g**: L-Ser(TBS). **5h**: L-Lys(Boc). **5i**: L-His(Boc). **5j**: L-Glu(*t*-Bu). **5k**: D-Phe], EDC·HCl, HOBt, DIPEA, CH_2Cl_2, rt, 2−4 h; (b) TFA/CH_2Cl_2/TIS/H_2O 48:49:2:1, rt, 2 h, [yields for two steps, for **6a** (L-Ala): 65%. **6b** (L-Leu): 59%. **6c** (L-Phe): 32%. **6d** (L-Pro): 41%. **6e** (L-Trp): 32%. **6f** (L-Tyr): 55%. **6g** (L-Ser): 43%. **6h** (L-Lys): 56%. **6i** (L-His): 10%. **6j** (L-Glu): 52%. **6k** (D-Phe): 31%].

experimental details). Compound **6e** obtained by this procedure was found to be spectroscopically and chromatographically identical to previously described inhibitor **6e** (whose stereochemistry was confirmed by X-ray crystallographic analysis),[11] which confirms both the stereochemical purity and identity of building block **4** used for the synthesis of inhibitors of type **6**.

For the structural diversification of P_1' position of phosphinic tripeptides, we employed a postmodification protocol[20] that has been successfully used in the past to the development of important inhibitors of various Zn metalloproteases.[14,17a,21] This protocol involves the application of a 1,3-dipolar cycloaddition reaction (1,3-DCR) between readily accessible nitrile oxides and an appropriate dipolarophilic precursor, such as tripeptide **9**, bearing a propargyl chain in P_1' position (Scheme 3). The synthesis of stereochemically pure precursors of similar type has been described by our group in the past;[20] therefore we decided to apply this chemistry to the preparation of compound **9**. Phosphinic acid **7** [$[\alpha]_D^{20}$ −41.3 (*c* 1, EtOH)] was prepared based on literature protocols[26] and subjected to a P-Michael addition with ethyl 2-methylenepent-4-ynoate as the electrophile. In accordance to previous observations,[17a,20] the reaction proceeded with a significant degree of diastereoselectivity (dr ≈ 2:1, based on ^{31}P NMR). Saponification and coupling of the resulting diacid **8** with phenylalanine carboxamide **5c** afforded **9** which allowed the efficient isolation of the major isomer **9** (*R,S,S*) after two recrystallizations by ethyl acetate in satisfactory overall yield. This stereochemically pure building block afforded inhibitors **13a−i** after application of the one-pot Huisgen protocol,[20] which involves the use of *N*-chlorosuccinimide (NCS) as an oxidant for the in situ generation of necessary nitrile oxides from the corresponding oximes,[27] and final acidic deprotection. Compound **13a** was resynthesized as a mixture of two epimers at P_1', **13a** (*R,S,S*) and **13a′** (*R,R,S*), by using the corresponding diastereoisomeric mixture of **9**. Inhibitor **13a** obtained from the stereocontrolled synthesis corresponds to the first RP-HPLC eluted isomer of the diastereoisomeric mixture obtained from the nonstereocontrolled synthesis. On the basis of previous studies which correlate the stereochemical configuration of P_1' position of phosphinic peptides with their elution order in RP-HPLC,[17a,19a,20] this is a strong indication of the *R,S,S* stereochemical assignment for propargylic precursor **9**. This was further supported after isolation of the two isomers by

DOI: 10.1021/acs.jmedchem.6b01031
J. Med. Chem. XXXX, XXX, XXX−XXX

Scheme 3. Synthesis of P_1' Isoxazole-Diversified Phosphinic Pseudotripeptide Inhibitors 13a–i[a]

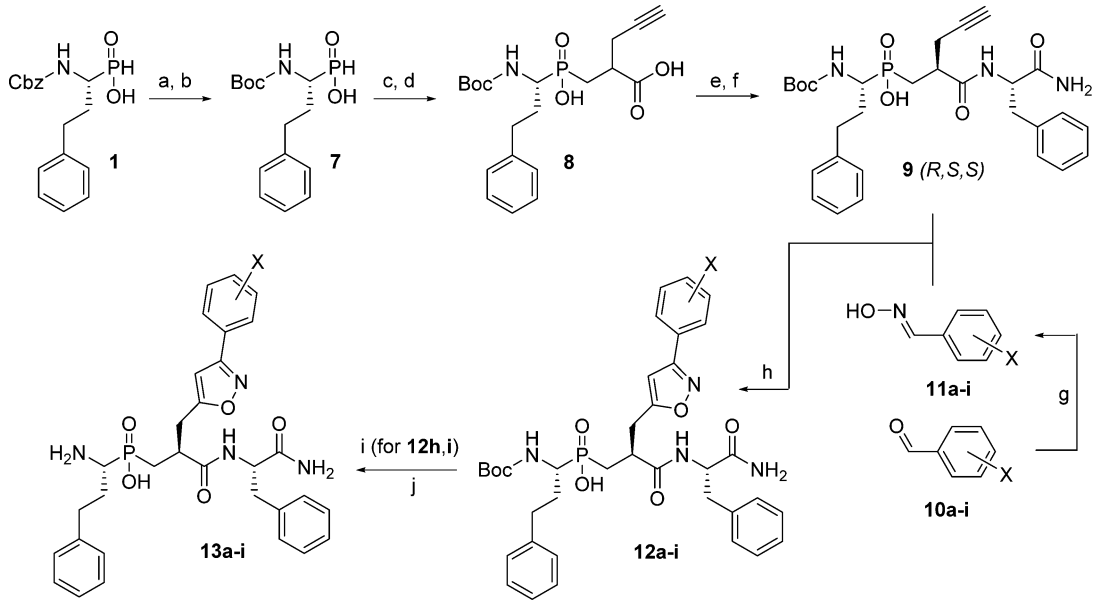

[a]Reagents and conditions: (a) 33% HBr/AcOH, rt, 1 h; (b) Boc_2O, Et_3N, DMF, rt, 24 h, 89%, two steps; (c) HMDS, $H_2C{=}C(CH_2C{\equiv}CH)COOEt$, 110 °C, 1 h, then 90 °C, 3 h, then EtOH, 70 °C, 30 min; (d) NaOH, MeOH, H_2O, rt, 24 h, then H_3O^+, 99%, two steps; (e) HBr·H-Phe-NH_2 (**5c**), EDC·HCl, HOBt, DIPEA, CH_2Cl_2, rt, 2 h; (f) recrystallization by AcOEt, 41%, two steps. (g) **10a–i** (X for **10a**: H. **10b**: *o*-OMe. **10c**: *m*-OMe. **10d**: *p*-OMe. **10e**: *o*-Cl. **10f**: *m*-Cl. **10g**: *p*-Cl. **10h**: *o*-OTBS. **10i**: *p*-OTBS). HCl·H_2NOH, CH_3COONa, MeOH, H_2O, rt, 24 h, 85–95%; (h) **11**, NCS, pyridine (cat.), $CHCl_3$, 45 °C, 3–4 h, then **9**, Et_3N, 45 °C, 3 d, 1–6 repetitions; (i) Cs_2CO_3, DMF/H_2O, rt, 2–3 d; (j) TFA/CH_2Cl_2/TIS/H_2O 48:49:2:1, rt, 2 h, two steps. For **13a**: 80%. **13b**: 85%. **13c**: 75%. **13d**: 76%. **13e**: 73%. **13f**: 67%. **13g**: 66%. **13h** (X = *o*-OH, three steps): 51%. **13i** (X = *p*-OH, three steps): 61%.

semipreparative RP-HPLC and evaluation of the inhibitory potency of individual isomers. Inhibition values showed that the first-eluted RP-HPLC-eluted isomer (**13a**) was 1–2 orders of magnitude more potent than its *R,R,S*-epimer (**13a′**) toward all aminopeptidases, a profile that is consistent with the higher potency observed for **6e** (possessing the stereochemical configuration of a natural substrate) as compared to its *R,R,S*-epimer **6e′**. Finally, inhibitor **14** was obtained by cleavage of the Boc group from **9**, using standard acidic deprotection conditions (Scheme 4).

Scheme 4. Synthesis of Phosphinic Inhibitor 14[a]

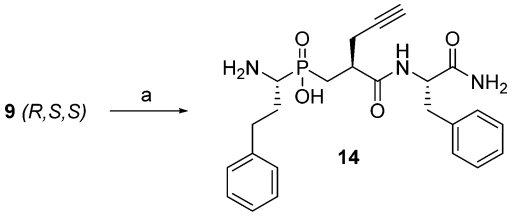

[a]Reagents and conditions: (a) TFA/CH_2Cl_2/TIS/H_2O 48:49:2:1, rt, 2 h, 87%.

Next, we proceeded to the synthesis of compounds **22a–f**, according to the general synthetic strategy outlined in Scheme 6. In particular, the synthesis of acrylic derivatives **15** and **19a,b** was initially performed as it is described in Scheme 5 (adamantyl-substituted acrylic ester **20** was prepared according to literature procedures[28]). Benzhydryl derivative **15** was prepared in good yield according to the protocol of Hin et al. which involves DCC-mediated coupling of 2,2-diphenylacetic acid with Meldrum's acid, reduction of the resulting enol,

Scheme 5. Synthesis of Acrylic Esters 15 and 19a,b[a]

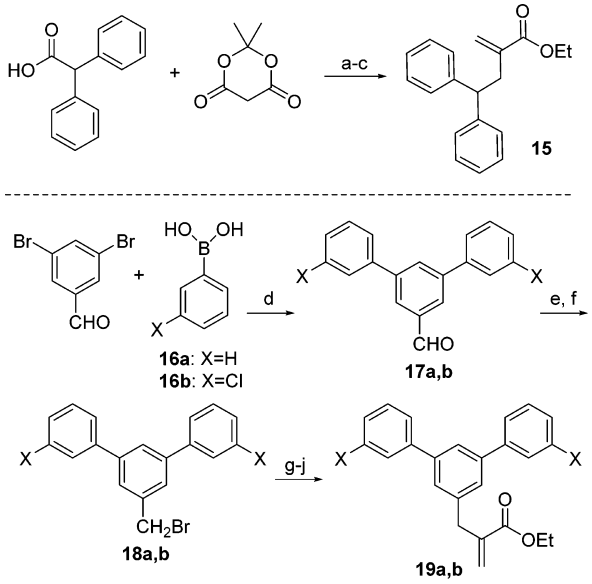

[a]Reagents and conditions: (a) DCC, DMAP, CH_2Cl_2, rt, 3 h; (b) $NaBH_4$, AcOH, CH_2Cl_2, rt, 24 h, 49%, two steps; (c) $[(CH_3)_2N{=}CH_2]I$, THF, EtOH, 65 °C, 24 h, 93%; (d) **16a**/**16b** $Pd(PPh_3)_4$, Na_2CO_3, DME, H_2O, 24 h. For **17a**: 98%. **17b**: 82%. (e) $NaBH_4$, EtOH, rt, 1.5 h; (f) PBr_3, CH_2Cl_2, rt 1 h, two steps. For **18a**: 91%. **18b**: 81%. (g) $HC(CO_2Et)_3$, K_2CO_3, DMF/toluene, reflux, 1.5 h; (h) KOH, EtOH, rt 24 h; (i) $(HCHO)_n$, Et_2NH, AcOEt, reflux, 4 h; (j) EtOH, EDC·HCl, DMAP, DIPEA, CH_2Cl_2, rt, 24 h, four steps. For **19a**: 56%. **19b**: 25%.

and final Mannich reaction using Eschenmosher's salt and EtOH as a scavenger of the ketene intermediate.[29] For the

DOI: 10.1021/acs.jmedchem.6b01031
J. Med. Chem. XXXX, XXX, XXX–XXX

Scheme 6. Synthesis of P_1' Diversified Phosphinic Pseudotripeptide Inhibitors 22a–f[a]

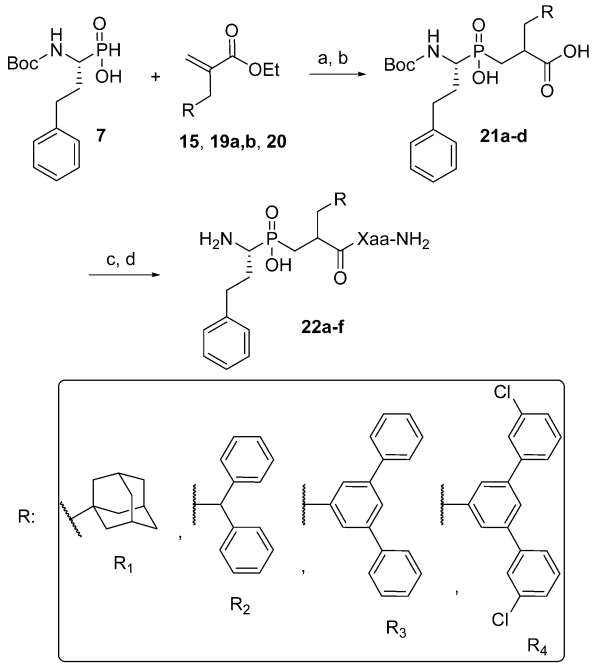

[a]Reagents and conditions: (a) HMDS, acrylic ester **15** or **19a,b** or **20** (R = 1-Ad), 110 °C, 1 h, then 90 °C, 3 h, then EtOH, 70 °C, 30 min; (b) NaOH, EtOH, H_2O, rt, 24 h, then H_3O^+, two steps. For **21a** (R = R_1): 79%. **21b** (R = R_2): 61%. **21c** (R = R_3): 88%. **21d** (R = R_4): 87%. (c) HBr·H-(L)Leu-NH_2 (**5b**) or HBr·H-(L)Phe-NH_2 (**5c**), EDC·HCl, HOBt, DIPEA, CH_2Cl_2, rt, 2–4 h; (b) TFA/CH_2Cl_2/TIS/H_2O 48:49:2:1, rt, 2 h, two steps,. For **22a** (R = R_1, Xaa = L-Phe): 79%. **22b** (R = R_2, Xaa = L-Phe): 80%. **22c** (R = R_2, Xaa = L-Leu): 75%. **22d** (R = R_3, Xaa = L-Phe): 78%. **22e** (R = R_3, Xaa = L-Leu): 65%. **22f** (R = R_4, Xaa = L-Leu): 40%.

synthesis of terphenyl derivatives **19a** and **19b**, aldehydes of type **17** were readily synthesized via Suzuki coupling of 3,5-dibromobenzaldehyde with the appropriate boronic acids.[30] The resulting aldehydes were converted to the corresponding bromides of type **18** after reduction with $NaBH_4$ and subsequent treatment with PBr_3. Substitution of the latter intermediates by the anion of triethyl methanetricarboxylate, followed by saponification/decarboxylation, Knoevenagel condensation of the crude substituted malonic acids with paraformaldehyde, and esterification of the resulting acrylic acids with EtOH successfully afforded the target acrylates **19**.[25,31] P-Michael addition of phosphinic acid **7** to acrylates **15**, **19a,b**, and **20** afforded dipeptides of type **21** as mixtures of two diastereoisomers with dr values ranging from 1:1 (**21a**) to 4:1 (**21d**). Coupling of **5b** or **5c** to diacids of type **21** followed by TFA-mediated deprotection afforded target compounds **22a–f**. For **22a,b** and **22d**, two isomers were obtained which were separated by semipreparative HPLC and evaluated separately (annotated as **22a′**, **22b′**, and **22d′** in Tables 1 and 2), whereas for **22c,e** and **22f** single isomers were obtained due to efficient separation during column purification of coupling products.

Structure–Activity Relationships: P_2' Position. Our first goal was to evaluate the effect of various proteinogenic amino acid side chains at P_2' position (with the only exception of **6k**) on the overall inhibition profile of APAs (Table 1). This side chain has been found to occupy the S_2' specificity pocket of ERAP2 in a previously determined crystal structure of

Table 1. In Vitro Evaluation of Phosphinic Pseudotripeptides 6a–k Varying at Position P_2'

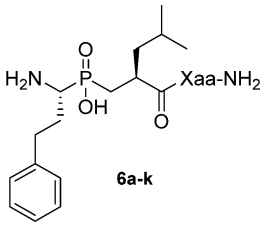

		IC_{50} (nM)		
compd	Xaa	ERAP1	ERAP2	IRAP
6a	L-Ala	2518 ± 390	96 ± 6	102 ± 9
6b	L-Leu	682 ± 40	118 ± 40	32 ± 2
6c	L-Phe	155 ± 38	109 ± 8	41 ± 6
6d	L-Pro	949 ± 236	144 ± 57	14 ± 1
6e	L-Trp	48 ± 16	80 ± 10	57 ± 35
6f	L-Tyr	340 ± 56	55 ± 7	29 ± 9
6g	L-Ser	7473 ± 1566	129 ± 11	1754 ± 631
6h	L-Lys	3093 ± 968	271 ± 55	1800 ± 411
6i	L-His	1969 ± 548	128 ± 23	381 ± 43
6j	L-Glu	2660 ± 174	243 ± 17	4024 ± 273
6k	D-Phe	2650 ± 212	211 ± 21	185 ± 5

ERAP2 with the inhibitor **6e**.[11] In vitro evaluation demonstrated that having aromatic residues at that position (**6c**, **6e**,**f**) is a prerequisite for retaining sufficient potency for ERAP1, although a small hydrophobic residue (**6b**) can also be well accommodated. Charged or hydrophilic residues (**6g–j**) greatly reduced the affinity for ERAP1 and so did the unnatural stereochemistry of P_2' in **6k**. In contrast, virtually all tested side chains could be well tolerated by ERAP2, leading to nanomolar inhibition for all compounds of type **6**, even for **6k** that possesses (*R*)-stereochemistry at P_2'. Hydrophobic side chains were also preferred by IRAP, in contrast to polar and charged residues that resulted in significantly reduced affinities. Overall, our analysis suggests that the P_2' position is more important for controlling inhibitor potency for ERAP1, less so for IRAP, and highly permissive for ERAP2. This comes largely as a surprise, since the crystal structure of ERAP2 with **6e** showed that the indole moiety of Trp at P_2' position is sandwiched between two Tyr residues that form the opposing sides of the S_2' pocket. One of these Tyr residues (Y438) is conserved in both ERAP1 and IRAP and is actually important for catalysis.[32] This apparent paradox can be rationalized by taking into account the conformational changes that ERAP1 (and probably ERAP2 and IRAP) undergoes during the catalytic cycle.[6b] ERAP1 has been crystallized in two distinct conformational states, a "closed" and an "open" state, as defined by the interactions between domains II and IV. The "open" state is considered to be less active and is characterized by disorder at the S_1 specificity pocket and a distinct conformation for the catalytic Y438. The "closed" state is correspondingly characterized by the lack of access of the catalytic site to the external solvent. Since any encounter complex between the inhibitor and ERAP1 would have to be with the "open" state, interactions that may facilitate the transition to the "closed" state which promotes the formation of the S_1 pocket would favor inhibitor affinity. It is conceivable therefore that aromatic side chains at P_2' may affect inhibitor affinity differently depending on the conformation of the catalytic Tyr residue. Indeed, the orientation of the catalytic Tyr is different among the three enzymes (Figure 2). The

DOI: 10.1021/acs.jmedchem.6b01031
J. Med. Chem. XXXX, XXX, XXX–XXX

Table 2. In Vitro Evaluation of Phosphinic Pseudotripeptides 13a−i, 14, and 22a−f Varying at Position P_1'

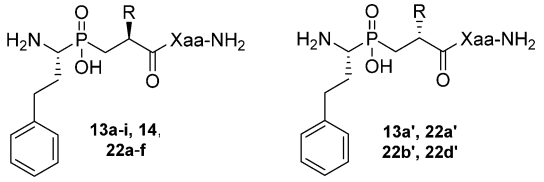

ID	R	Xaa	IC_{50} (nM)		
			ERAP1	ERAP2	IRAP
13a	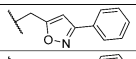	L-Phe	126±31	190±24	18±3
13a′	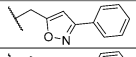	L-Phe	2087±347	878±334	434±50
13b	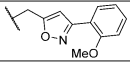	L-Phe	178±67	130±15	13±2
13c	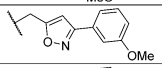	L-Phe	98±11	217±76	20±4
13d	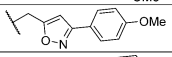	L-Phe	48±9	84±21	10±2
13e	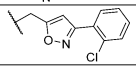	L-Phe	102±11	123±14	13±4
13f	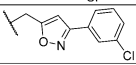	L-Phe	143±14	225±67	41±5
13g	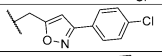	L-Phe	71±8	345±138	34±9
13h	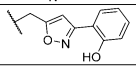	L-Phe	65±38	83±11	9±2
13i	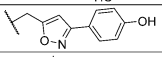	L-Phe	33±5	56±9	4±1
14		L-Phe	43±4	37±4	2±1
22a		L-Phe	726±157	412±89	46±17
22a′		L-Phe	27008±7715	2271±486	561±66
22b		L-Phe	3694±908	740±129	32±9
22b′		L-Phe	>100000	1922±199	221±24
22c		L-Leu	31212±6939	246±7	16±2
22d		L-Phe	>35000	105±15	21±3
22d′	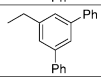	L-Phe	>100000	4622±2517	281±100
22e	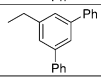	L-Leu	21229±907	2565±47	317±20
22f	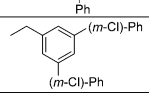	L-Leu	25111±6363	13814±566	577±21

importance for aromatic residues at P_2' appears to correlate well with the known orientation of this Tyr (most important for ERAP1, less so for IRAP, and not important for ERAP2). These observations suggest that SAR for inhibitors that occupy the S_2' pocket of APAs these enzymes may be complicated by the conformational states available to each enzyme.

Structure−Activity Relationships: P_1' Position. Evaluation of the P_1' position was performed along two separate routes involving (a) isoxazole-based, linearly extended side chains (**13a−i**) to explore the depth of S_1' pocket and (b) "expanded" bulky side chains (**22a−f**) to explore the base of the same pocket. Our results showed that the bulky side chains of inhibitors **22a−f** were poorly tolerated by ERAP1 whereas

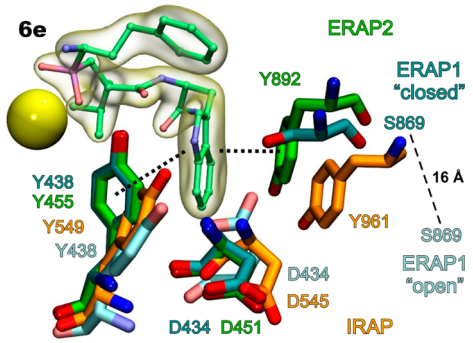

Figure 2. Three key residues that comprise the S_2' subsite of APAs. The X-ray crystal structure of ERAP2 complex with **6e** (green C, PDB code 4JBS) is superimposed with ERAP1 complexes with bestatin (PDB codes 2YD0, 3MDJ) in the closed and open states (dark and light cyan C, respectively), and IRAP in its ligand-free form (orange C, PDB code 5C97). Note the different orientations of the catalytic Y438, the conserved D434, and the nonconserved S869, especially in the open and closed states of ERAP1.

the extended isoxazole side chains of **13h,i** were well tolerated (Table 2). A similar but less striking phenomenon was evident for ERAP2, albeit with some notable exceptions, such as **22d**. In contrast, IRAP was able to easily accommodate the P_1' side chains of both groups of compounds (**13h,i** and **22a−f**), resulting in most cases in low nanomolar inhibition. This was more evident in the case of linear isoxazole side chains, considering that all inhibitors of type **13** were able to potently inhibit IRAP with IC_{50} values ranging between 4 and 41 nM. The ability of IRAP to accommodate bulky side chains at P_1' position may be explained by the different orientation that the conserved GAMEN motif adopts in this enzyme, an orientation that allows for a more open catalytic site and has been hypothesized to allow processing of cyclic peptides that may also require additional space around the base of S_1' pocket.[5c] Interestingly, inversion of the stereochemical configuration at P_1' position caused a dramatic drop in the potency of all examples presented in Table 2 (**13a′**, **22a′**, **22b′**, and **22d′**), which is consistent with previously reported observations for the pair of P_1'-epimers **6e** and **6e′**[11] and emphasizes the importance of stereochemical control in the development of optimized inhibitors of APAs, in terms of both potency and selectivity.

Critical Parameters for Maximizing Potency. As it is demonstrated in Tables 1 and 2, the potency of phosphinic tripeptide inhibitors against ERAP1 can be greatly affected by both P_1' and P_2' side chain composition. Aromatic residues are preferred at P_2' position presumably due to the importance of interaction with Y438 that facilitates the conformational change to the closed form of the enzyme. Long side chains at P_1' position, such as the aryl-substituted isoxazole derivatives **13a−i**, are well accommodated but do not confer any additional affinity compared to a small hydrophobic residue (such as Leu, **6b**) at the same position. In contrast, bulky substituents are highly disfavored at P_1' position.

The effectiveness of phosphinic tripeptides against ERAP2 was found to be highly permissive with respect to position P_2', since all compounds exhibited activity in the nanomolar range (with the exception of **22e**, **22f**, and all primed diastereoisomers listed in Table 2). Similar to ERAP1, bulky residues at P_1' position may not be optimal but are well tolerated and in some cases can result in highly potent inhibitors (such as **22d**).

DOI: 10.1021/acs.jmedchem.6b01031
J. Med. Chem. XXXX, XXX, XXX−XXX

P_2' position is also important for potency against IRAP: polar and charged residues lead to reduction of the affinity, presumably reporting a hydrophobic environment for subsite S_2'. Inhibitor potency was also affected by the nature of the P_1' side chain, especially for bulky substituents, but in general IRAP was able to accommodate bulky side chains while retaining nanomolar potency.

The affinity displayed by inhibitor **14** that bears a propargyl group at P_1' position is also highly notable, since it appears to outperform leucine (**6c**) for all enzymes and especially IRAP, resulting in an IC_{50} value of 2 nM. This affinity is in the same range as for several macrocyclic angiotensin IV analogues developed by Hallberg and co-workers which are among the most potent known IRAP inhibitors.[33] Moreover, to the best of our knowledge, **14** is the most potent inhibitor of ERAP2 described to date (IC_{50} = 37 nM) and parallels **6e** for potency against ERAP1 (IC_{50} = 43 nM for **14** and IC_{50} = 48 nM for **6e**). Although the origin of this outstanding behavior is not clear, putative interactions between the electron-rich triple bond of the propargyl group and the catalytic Zn(II) atom at certain orientations may provide a reasonable explanation.[34] Given the absence of any literature precedent concerning propargyl substituted phosphinic inhibitors of Zn metallopeptidases, further investigations including crystallographic analysis will be necessary to clarify this effect.

Critical Parameters for Maximizing Selectivity. Our screening results revealed several compounds to be selective inhibitors of ERAP2 and IRAP with respect to ERAP1 but afforded only few compounds displaying selectivity for ERAP1, consistent with previous reports (Figure 3).[10b,11,35] This is likely a result of the conformational dynamics of ERAP1, which samples more open states than ERAP2 and IRAP with partially disordered S_1 and S_2' subsites, rendering inhibitor targeting quite challenging.[6c,10b] Still, some selectivity was evident for some of the isoxazole derivatives, indicating that the P_1' position can be valuable in enhancing ERAP1 selectivity over ERAP2. For example, compound **13g** is about 5-fold more selective for ERAP1 versus ERAP2. In an attempt to rationalize this observation, we examined the predicted conformations of **13g** from docking calculations, which showed that the P_1' side chain extends in a linear fashion down the elongated shallow S_1' pocket of ERAP1 (Figure 4A). This pocket is much shallower in ERAP2 (Figure 4B), making this conformation inaccessible to extended P_1' side chains and possibly explaining the observed selectivity. Another informative observation that supports the aforementioned shape description of S_1' subsite for ERAP1 and ERAP2 is the fact that among the isoxazole series, ortho-substituted aryl substituents (**13b**, **13e**, and **13h**) result in the least ERAP1-selective compounds (in fact, **13b** bearing the bulkier −OMe group displays higher potency for ERAP2 than ERAP1). Evidently, in contrast to **13g**, inhibitors **13b**, **13e**, and **13h** require a wider, more spacious S_1' channel for favorable accommodation of their P_1' side chains, which results in reduction of their affinity for ERAP1.

Both P_1' and P_2' side chains of phosphinic tripeptides offer opportunities for the optimization of ERAP2 selective inhibitors. Screening of P_2' position resulted in several compounds that were selective for ERAP2 over ERAP1 (Figure 3A). In particular, polar and charged side chains were well tolerated by ERAP2 but not ERAP1, thus providing selective inhibitors, such as **6g** that exhibits 50-fold selectivity for ERAP2. In regard to the P_1' position, some of the bulky side chains that were tolerated by ERAP2 resulted in highly selective

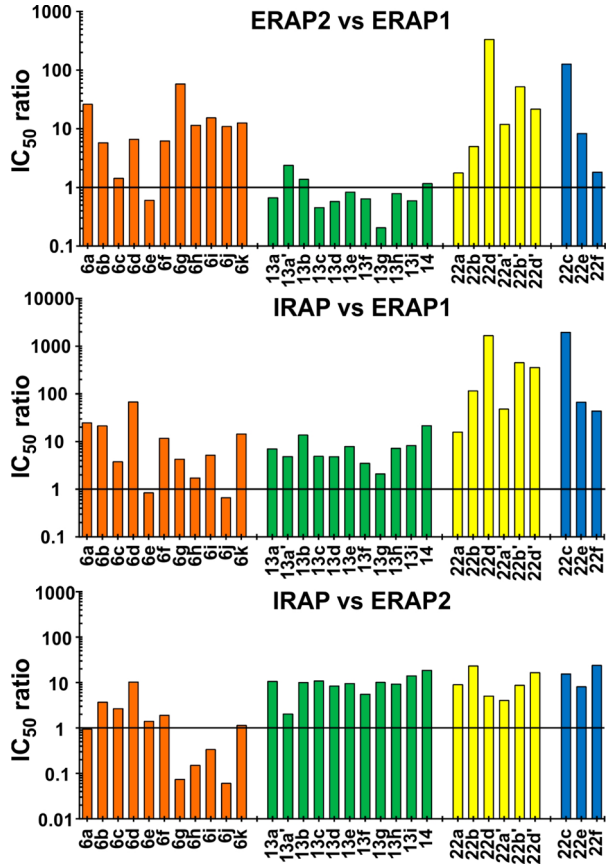

Figure 3. Ratio of IC_{50} values showing the selectivity of phosphinic tripeptide inhibitors (A, top) for ERAP2 over ERAP1, (B, middle) IRAP over ERAP1, and (C, bottom) IRAP over ERAP2.

inhibitors. For example, **22d** was found to be over 350-fold selective for ERAP2 over ERAP1. Docking calculations suggest that **22d** binds to ERAP2 with the P_1' side chain abutting to the extension of the GAMEN loop (Figure 5). At this site, the presence of two nonconserved residues in ERAP1 (Q315 and S316) that could interfere with this configuration of **22d** possibly accounts for the observed selectivity.

The highest selectivity during our screening analysis was observed for IRAP, with several derivatives reaching selectivity of over 3 orders of magnitude (Figure 2). This was true for screening of both the P_1' and P_2' positions with respect to ERAP1 but only for the P_1' position with respect to ERAP2. Taken together, the P_1' position proved to be an exceptional modification site for generating IRAP-selective inhibitors. This ability of IRAP to accommodate in its S_1' subsite very bulky groups justifies the nanomolar affinity for IRAP observed by all listed compounds of Table 2. In fact, this feature is more striking in IRAP than in ERAP2, considering that in the most extreme case of bulky P_1' side chain (**22f**) examined in this work, nanomolar affinity for IRAP was still attainable (IC_{50} = 577 nM) whereas IC_{50} value for ERAP2 was dramatically increased to 13 μM. This may be due to the alternative configuration of the GAMEN loop in IRAP that generates additional space around that site, making it more permissive, especially for bulky side chains. In an effort to put these observations under a structural perspective we docked IRAP-selective inhibitor **22b** in the active site of IRAP. Two major low-energy configurations were identified and shown in Figure 6. Interestingly, in both configurations the P_1' side chain does

DOI: 10.1021/acs.jmedchem.6b01031
J. Med. Chem. XXXX, XXX, XXX−XXX

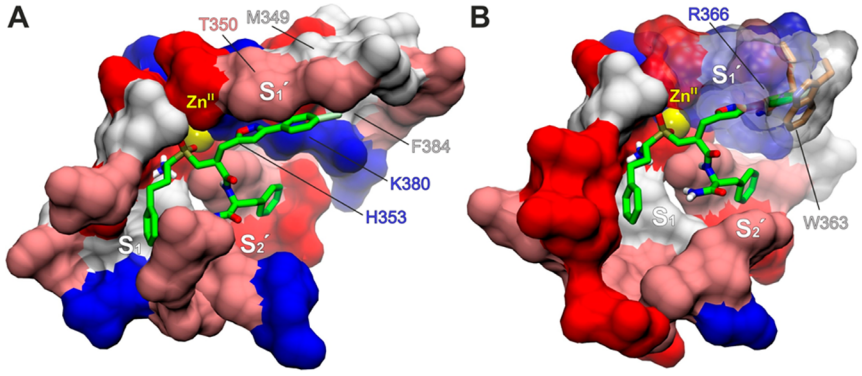

Figure 4. (A) Docked conformation of **13g** in the active site of ERAP1 (PDB code 2YD0), where the P1′ side chain extends inside the deep, elongated S_1' pocket. (B) Active site of ERAP2 (PDB code 4JBS) shown from an identical view, where the shallower S_1' subsite renders such an extended configuration of **13g** inaccessible due to steric clashes with R366 and W363. Colors are as in Figure 1.

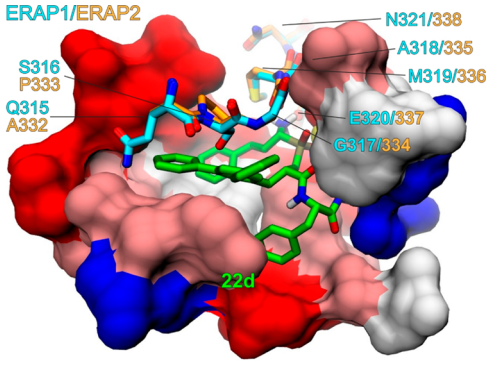

Figure 5. Lowest energy conformation of **22d** (green C) docked inside the active site of ERAP2 (orange C), superimposed with ERAP1 (cyan C) to illustrate the conserved GAMEN motif and the two nonconserved preceding residues that probably restrict the accommodation of similar conformations of **22d** in ERAP1 (PDB codes 2YD0 for ERAP1, 4JBS for ERAP2).

not interact with the GAMEN-motif residues but rather forces either the P_1 or P_2' side chain to occupy the free space adjacent to the GAMEN loop. This space is not readily available in ERAP1, making these configurations inaccessible (Figure 6).

Biological Evaluation. To access the efficacy and selectivity of this group of inhibitors in regulating antigenic peptide processing in live cells, we evaluated the ability of one of the IRAP-selective inhibitors, **22b** (DG026A), to regulate cross-presentation by dendritic cells (DCs) as described in the Experimental Section. DCs can perform cross-presentation by at least two distinct pathways, one of which is dependent on ERAP1 activity and the other is dependent on IRAP activity.[4a] To confirm the selectivity of any effect, we compared BMDCs from both wild-type and IRAP$^{-/-}$ knockout mice. Mouse CD8α^+ and CD11b$^+$ DCs were exposed to soluble ovalbumin (OVA) in the presence of increasing concentrations of the inhibitor. After 6 h the cells were fixed to stop antigen processing and mixed with CD8$^+$ T-cells isolated from the lymph nodes of Rag-1$^{-/-}$ C57Bl/6 OT-I mice. T-cell activation was evaluated by measuring the levels of secreted IL-2 by the activated CD8$^+$ T-cells. The OT-I T cell response to increasing levels of soluble OVA (Figure S1) was first evaluated to determine the optimal concentration of OVA for all subsequent experiments (set to 500 μg/mL) (Figure S1). For both CD8α^+ and CD11b$^+$ DCs, titration of the inhibitor **22b** resulted in a dose-dependent reduction of cross-presentation down to a plateau that corresponds to IRAP-independent cross-presentation (Figure 7A). No effect was evident when using DCs isolated from IRAP$^{-/-}$ knockout mice, indicating that the effect was IRAP-specific (Figure 7B). A limited additional effect was seen at the highest inhibitor concentration (3.3 μM) which may be attributable to toxicity. In conclusion, we demonstrate a dose-dependent and target-specific effect of the IRAP selective inhibitor **22b** on the cross-presentation by both subsets of conventional DCs, which indicates that this compound may be useful in regulating DC-triggered adaptive immune responses.

CONCLUSIONS

In this study, we expanded on our previous observation that phosphinic pseudotripeptides are potent inhibitors of aminopeptidases that are involved in the generation of antigenic

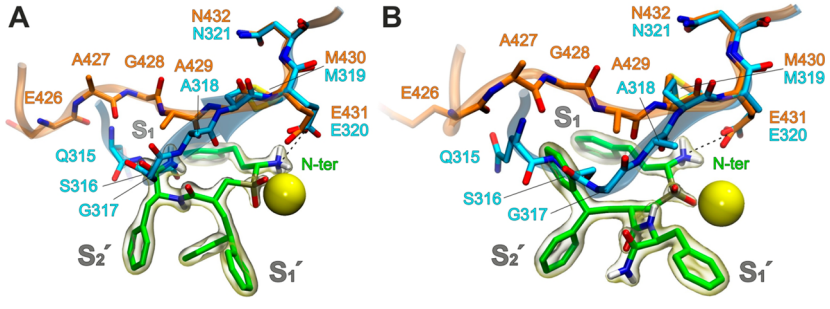

Figure 6. Two docked conformations of **22b** (green C) inside the active site of IRAP (orange C), superimposed with the structure of closed ERAP1 (cyan C). The more "closed" configuration of the GAMEN motif and of the two preceding residues in ERAP1 with respect to IRAP probably renders such bound poses of **22b** inaccessible (PDB codes 2YD0 for ERAP1, 5C97 for IRAP).

DOI: 10.1021/acs.jmedchem.6b01031
J. Med. Chem. XXXX, XXX, XXX−XXX

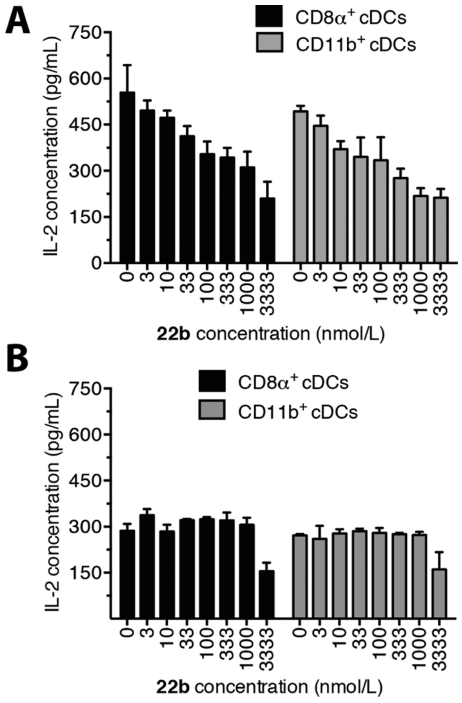

Figure 7. Response of $CD8^+$ T-cells isolated from the lymph nodes of Rag-$1^{-/-}$ C57Bl/6 OT-I mice to FACS-sorted splenic $CD8\alpha^+$ and $CD11b^+$ conventional DCs exposed to soluble OVA in the presence of the inhibitor **22b**. DCs were isolated either from wild-type (A) or from $IRAP^{-/-}$ knockout mice (B). A dose-dependent inhibition of the response by DCs from wild-type mice is evident (A) down to the level of activation seen for DCs isolated from knockout mice (B).

peptides, by thoroughly investigating the P_1' and P_2' positions for their effect on inhibitor potency and selectivity. Special attention was given to the control of chirality during the preparation of target compounds, considering the difference in affinity of 2−3 orders of magnitude previously observed for the P_1'-epimers **6e** and **6e′** and verified in this study for several more cases of phosphinic tripeptides. This requirement is of paramount importance for the accurate evaluation of reported structure−activity relationships and the discovery of improved inhibitors, especially in terms of selectivity. In this regard, appropriately adjusted synthetic plans able to confer stereochemical control were devised and employed. Our strategy succeeded in providing several low nanomolar inhibitors for all APAs, such as **14** which is among the most potent inhibitors ever reported for all three enzymes. Important inhibitors in terms of selectivity have also been identified, such as the ERAP2 selective inhibitor **6g** and the IRAP selective inhibitor **22b**. Our analysis suggests that the P_2' position is more important for controlling inhibitor potency for ERAP1 than for ERAP2 and IRAP. Moreover, selectivity for ERAP2 can be controlled by polar residues at P_2' position while selectivity for IRAP is mainly determined by the presence of bulky groups at P_1' position. A notable observation concerning the effect of shape of P_1' side chains in ERAP1/ERAP2 selectivity is that ERAP1 accommodates better than ERAP2 long, linear ligands whereas this preference is inversed in the case of more "expanded" bulky groups (e.g., **22d**). Biological evaluation demonstrated that one of the selective IRAP inhibitors (**22b**) was able to regulate cross-presentation by dendritic cells ex vivo in a dose-dependent and target-specific fashion. Our results suggest that this class of compounds can be useful for the targeted regulation of adaptive immune responses and encourage their preclinical evaluation for applications in cancer immunotherapy or the control of autoimmunity. Possible bioavailability concerns associated with the high polarity of the described structures can be overcome either by prodrug-based strategies, as it has been successfully demonstrated in the past with fosinopril,[36] a known marketed phosphinic inhibitor of angiotensin-converting enzyme, and with a series of structurally relevant phosphinic inhibitors of NEP and APN (aminopeptidase N) that exhibit analgesic properties,[22a] or with intravenous (iv) or intraperitoneal (ip) administration to animals.

EXPERIMENTAL SECTION

Materials and General Procedures. Solvents for reactions were purchased as anhydrous grade and stored over 4 Å activated molecular sieves before use. Reagents were purchased from commercial sources and were used without further purification. Column chromatography was performed on silica gel (E. Merck, 70−230 mesh). TLC analyses were performed on silica gel plates (E. Merck, silica gel 60 F254), and components were visualized by the following methods: UV light absorbance, ninhydrin spraying and/or charring after spraying with a solution of NH_4HSO_4. Coupling reactions were monitored by LC/MS analysis. Melting points (measured on an Electrothermal apparatus) are uncorrected. Optical rotation data were acquired on a PerkinElmer 343 polarimeter at 25 °C. NMR spectra were recorded on a Varian 200 MHz Mercury or a Bruker Avance DRX-500 instrument at 25 °C. ^1H and ^{13}C spectra are referenced according to the residual peak of the solvent based on literature data.[37] ^{31}P NMR chemical shifts are reported in ppm downfield from 85% H_3PO_4 (external standard), and the corresponding spectra are fully proton decoupled. The following abbreviations are used to designate the multiplicities: s, singlet; d, doublet; t, triplet; q, quartet; m, multiplet; br, broad. ESI mass spectral analysis was performed on a MSQ Surveyor, Finnigan mass spectrometer, using direct sample injection. Negative or positive ion ESI spectra were acquired by adjusting the needle and cone voltages accordingly. HRMS spectra were recorded on a Bruker Maxis Impact QTOF spectrometer or a 4800 MALDI-TOF mass spectrometer (Applied Biosystems, Foster City, CA, USA) in positive reflectron mode in the m/z range of 100−700. Each spectrum was the result of 1000−2000 shots (20 different positions into each spot and 50 shots per subspectrum), and internal calibration was applied by using 4-HCCA matrix m/z. Stereochemical purity of intermediates and final inhibitors was determined using ^{31}P NMR and/or RP-HPLC analysis. RP-HPLC analyses were performed on a Hewlett-Packard 1100 model (C18-Cromasil-RP, 5 μm, UV/vis detector, flow of 0.5 mL/min, 254 and/or 280 nm detection). Conditions and gradients used for each compound are reported in Supporting Information. Purity of compounds after preparative reverse-phase HPLC was assessed by analytical HPLC (Merck Chromolith C-18 column) using a 0.05% TFA−acetonitrile gradient (5−40%). On the basis of these criteria, all compounds possess purity of >95%.

General Procedure A: P-Michael Addition of P−H Phosphinic Acids to Acrylic Derivatives. A mixture of the appropriate N-protected aminophosphinic acid (1.0 mmol), the appropriate acrylic derivative (1.1−1.5 mmol), and HMDS (1.05 mL, 5.0 mmol) was heated at 110 °C for 1 h and then at 90 °C for 3 h under Ar. Then, the mixture was slowly cooled at 70 °C, dry EtOH (1.5 mL) was slowly added, and the resulting mixture was stirred at 70 °C for 20 min. After removal of the volatiles in vacuo, the residue was taken up by AcOEt (20 mL) and the organic solution was washed with 2 M HCl (2 × 10 mL) and brine (10 mL). The organic layer was dried over Na_2SO_4 and evaporated in vacuo to afford the crude product. Purification details are described for each case separately.

General Procedure B: Saponification of P-Michael Adducts. The appropriate P-Michael addition product (1.0 mmol) was dissolved in EtOH (10 mL), and the solution was cooled to 0 °C. 1 M NaOH (5 mL) was added portionwise, and the mixture was stirred at rt for 24 h.

DOI: 10.1021/acs.jmedchem.6b01031
J. Med. Chem. XXXX, XXX, XXX−XXX

After removal of the volatiles in vacuo, the residue was suspended in H_2O (10 mL) and AcOEt (20 mL) and acidified with 2 M HCl to pH 1. The aqueous phase was extracted twice more with AcOEt (2 × 10 mL), and the combined organic layers were dried over Na_2SO_4 and evaporated in vacuo.

General Procedure C: TFA-Mediated Deprotection of Final Inhibitors. A solution of the appropriate protected pseudopeptide (0.2 mmol) in TFA/CH_2Cl_2/TIS/H_2O 48:49:2:1 (2 mL) was stirred at rt for 2 h. After removal of the volatiles in vacuo, the residue was dried azeotropically using toluene, and then it was treated with dry Et_2O at 0 °C. The precipitate was collected by centrifugation, washed twice with dry Et_2O, and dried over P_2O_5 to afford the final product.

General Procedure D: Coupling of Amino acid Carboxamides to Phosphinic Building Blocks. The appropriate phosphinic pseudodipeptide building block (0.5 mmol) was suspended/dissolved in CH_2Cl_2 (1.0 mL) and DIPEA (174 μL, 1.0 mmol), and the appropriate amino acid carboxamide (0.65 mmol), HOBt (68 mg, 0.5 mmol), and EDC·HCl (480 mg, 2.5 mmol) were added. The mixture was stirred at rt and the reaction was monitored by TLC until complete consumption of the starting phosphinic acid (2−4 h). Then, the solvent was evaporated, AcOEt (10 mL) and 1 M HCl (10 mL) were added, and the organic layer was separated and washed with 1 M HCl (3 × 10 mL), H_2O (5 mL), and brine (5 mL). The organic phase was dried over Na_2SO_4, evaporated in vacuo and the residue was purified by column chromatography ($CHCl_3$/MeOH/AcOH 7:0.1:0.1 → 7:0.5:0.5) to afford the target protected pseudotripeptide.

General Procedure E: 1,3-Dipolar Cycloaddition toward the Synthesis of Isoxazole Inhibitors. The appropriate oxime (3.0 mmol) was dissolved in $CHCl_3$ (10 mL), and 2 drops of pyridine were added. Then, NCS (401 mg, 3.0 mmol) was added at rt, and after 10 min the resulting mixture was stirred at 40−50 °C for 3 h. In this solution, phosphinic tripeptide **13** (167 mg, 0.3 mmol) was added, followed by slow addition of Et_3N (0.49 mL, 3.5 mmol) at the same temperature. The reaction mixture was stirred for 3 days at 40−50 °C. Then, the solvent was evaporated, AcOEt (10 mL) and 1 M HCl (10 mL) were added, and the organic layer was separated and washed with 1 M HCl (3 × 10 mL), H_2O (5 mL), and brine (5 mL). The organic phase was dried over Na_2SO_4 and evaporated in vacuo. In case of incomplete reaction, the procedure was repeated as many times as necessary using the product of each reaction as starting material for the next reaction. When the starting material was fully consumed, the crude product was purified by column chromatography ($CHCl_3$/MeOH/AcOH 7:0.1:0.1 → 7:0.5:0.5) to afford the target isoxazole pseudotripeptide.

((1*R*)-1-{[(Benzyloxy)carbonyl]amino}-3-phenylpropyl)[2′-(ethoxycarbonyl)-4′-methylpentyl]phosphinic Acid (2). Phosphinic acid **1** (7.0 g, 21 mmol) was converted to compound **2** according to general procedure A. The crude product was used at the next step without further purification. For analytical reasons, a small sample was purified by column chromatography ($CHCl_3$/MeOH/AcOH 7:0.1:0.1 → 7:0.5:0.5) to afford compound **2** as a white solid. ^{1}H NMR (200 MHz, DMSO-d_6/2% TFA) δ 0.79 (t, *J* = 6.5 Hz, 6H), 1.11 (t, *J* = 7.0 Hz, 3H), 1.18−1.51 (m, 3H), 1.52−2.09 (m, 4H), 2.31−2.88 (m, 3H), 3.48−3.78 (m, 1H), 4.00 (q, *J* = 6.8 Hz, 2H), 5.06 (s, 2H), 7.04−7.42 (m, 10H), 7.62 (d, *J* = 9.6 Hz, 1H); ^{13}C NMR (50 MHz, $CDCl_3$) δ 14.2, 22.0, 22.8, 25.9, 28.8 (d, $^1J_{PC}$ = 85.4 Hz), 29.3 (d, $^1J_{PC}$ = 90.7 Hz), 29.9, 32.0, 32.1, 32.2, 32.3, 37.2, 37.3, 43.2, 43.3, 43.4, 43.6, 49.2 (d, $^1J_{PC}$ = 104 Hz), 50.1 (d, $^1J_{PC}$ = 104 Hz), 60.9, 67.3, 125.4, 126.2, 128.1, 128.2, 128.5, 128.6, 129.1, 136.4, 136.5, 140.9, 140.9, 156.3, 156.4, 175.2, 175.3, 175.4; ^{31}P NMR (81 MHz, DMSO-d_6) δ 45.7, 46.0. ES-MS *m*/*z*: calcd for $[C_{26}H_{36}NO_6P - H]^-$ 488.2; found, 488.2. HRMS (*m*/*z*): $[M + Na]^+$ calcd for $C_{26}H_{36}NNaO_6P^+$, 512.2172; found, 512.2178.

(2′*S*)-2′-{[((1*R*)-1-{[(Benzyloxy)carbonyl]amino}-3-phenylpropyl)(hydroxy)phosphoryl]methyl}-4′-methylpentanoic Acid (3). The crude product **2** from the above preparation was subjected to saponification according to general procedure B. The resulting crude product was recrystallized twice by AcOEt to afford compound **3** as a white solid (4.45 g, 46% starting from **1**). Mp 160−162 °C; ^{1}H NMR (200 MHz, DMSO-d_6/2% TFA) δ 0.82 (t, *J* = 5.9 Hz, 6H), 1.20−2.09 (m, 7H), 2.36−2.83 (m, 3H), 3.50−3.72 (m, 1H), 5.07 (s, 2H), 7.04−7.42 (m, 10H), 7.63 (d, *J* = 9.4 Hz, 1H); ^{13}C NMR (50 MHz, DMSO-d_6) δ 21.8, 23.0, 25.6, 28.9 (d, $^1J_{PC}$ = 88.2 Hz), 29.2, 29.3, 31.5, 31.8, 36.7, 36.8, 42.6, 42.7, 50.4 (d, $^1J_{PC}$ = 105.9 Hz), 65.6, 126.0, 127.7, 127.9, 128.4, 128.5, 128.5, 137.3, 141.3, 156.4, 156.4, 176.4, 176.5; ^{31}P NMR (81 MHz, DMSO-d_6/3% TFA) δ 47.3. ES-MS *m*/*z*: calcd for $[C_{24}H_{32}NO_6P - H]^-$ 460.2; found, 460.2. HRMS (*m*/*z*): $[M + H]^+$ calcd for $C_{24}H_{33}NO_6P^+$, 462.2040; found, 462.2046.

(2′*S*)-2′-{[((1*R*)-1-{[(*tert*-Butoxy)carbonyl]amino}-3-phenylpropyl)(hydroxy)phosphoryl]methyl}-4′-methylpentanoic acid (4). A solution of compound **3** (4 g, 8.7 mmol) in 33% HBr/AcOH (7 mL) was stirred at rt for 1 h. After removal of the volatiles in vacuo, the residue was dried azeotropically using toluene and then it was dissolved in DMF (20 mL). To this solution, Et_3N (6.0 mL, 43 mmol) and $(Boc)_2O$ (2.3 g, 10.4 mmol) were added at 0 °C, and the final mixture was stirred at rt for 24 h. Then, the mixture was diluted with AcOEt (100 mL) and 1 M HCl (100 mL) and the organic phase was washed with 1 M HCl (2 × 20 mL), H_2O (2 × 20 mL), and brine (10 mL). The organic phase was dried over Na_2SO_4 and evaporated in vacuo. The residue was dissolved in 5% $NaHCO_3$ (70 mL), washed with Et_2O (3 × 10 mL), and acidified with 1 M HCl to pH 1. The aqueous suspension was extracted with AcOEt (2 × 30 mL) and the organic layers were dried over Na_2SO_4 and evaporated under vacuum to afford compound **4** as a white solid (3.4 g, 92%). Mp 128−132 °C; ^{1}H NMR (200 MHz, DMSO-d_6/2% TFA) δ 0.83 (t, *J* = 5.9 Hz, 6H), 1.38 (s, 9H), 1.05−1.58 (m, 3H), 1.60−2.13 (m, 4H), 2.35−2.79 (m, 3H), 3.35−3.64 (m, 1H), 7.02−7.33 (m, 5H); ^{13}C NMR (50 MHz, DMSO-d_6) δ 22.0, 23.2, 25.8, 28.4, 29.0 (d, $^1J_{PC}$ = 89.7 Hz), 29.3, 31.8, 32.0, 36.9, 37.0, 42.6, 42.8, 49.8 (d, $^1J_{PC}$ = 105.2 Hz), 78.6, 126.1, 128.5, 128.7, 141.5, 155.9, 156.0, 176.6, 176.8; ^{31}P NMR (81 MHz, DMSO-d_6) δ 46.8. ES-MS *m*/*z*: calcd for $[C_{21}H_{34}NO_6P - H]^-$ 427.2; found, 426.2. HRMS (*m*/*z*): $[MNa]^+$ calcd for $C_{21}H_{34}NNaO_6P$ 450.2016; found, 450.2022.

((1*R*)-1-Amino-3-phenylpropyl){(2′*S*)-2′-[((2″*S*)-1″-amino-1″-oxopropan-2″-yl)carbamoyl]-4′-methylpentyl}phosphinic Acid (6a). Coupling of **4** with H-(L)Ala-NH_2 (**5a**) according to general procedure D and subsequent deprotection according to general procedure C afforded compound **6a** as a white solid (yield for two steps: 65%). ^{1}H NMR (200 MHz, DMSO-d_6/2% TFA) δ 0.84 (dd, *J* = 5.7, 11.4 Hz, 6H), 1.19 (d, *J* = 7.1 Hz, 3H), 1.14−1.50 (m, 3H), 1.70−2.23 (m, 4H), 2.56−2.90 (m, 3H), 3.11−3.37 (m, 1H), 4.15 (quint, *J* = 7.1 Hz, 1H), 6.81−7.58 (m, 7H), 8.09 (d, *J* = 7.4 Hz, 1H), 8.25 (br s, 3H); ^{13}C NMR (50 MHz, DMSO-d_6/2% TFA) δ 18.1, 22.4, 22.9, 25.2, 29.7 (d, $^1J_{PC}$ = 91.8 Hz), 29.7, 31.6, 31.8, 37.7, 37.7, 43.2, 43.4, 48.5, 48.7 (d, $^1J_{PC}$ = 93.8 Hz), 126.4, 128.5, 128.7, 141.0, 173.9, 174.0, 174.6; ^{31}P NMR (81 MHz, DMSO-d_6) δ 41.7. HRMS (*m*/*z*): $[M - H]^-$ calcd for $C_{19}H_{31}N_3O_4P^-$, 396.2058; found, 396.2059.

((1*R*)-1-Amino-3-phenylpropyl){(2′*S*)-2′-[((2″*S*)-1″-amino-4″-methyl-1″-oxopentan-2″-yl)carbamoyl]-4′-methylpentyl}-phosphinic Acid (6b). Coupling of **4** with HBr·H-(L)Leu-NH_2 (**5b**) according to general procedure D and subsequent deprotection according to general procedure C afforded compound **6b** as a white solid (yield for two steps: 59%). ^{1}H NMR (200 MHz, DMSO-d_6/2% TFA) δ 0.67−0.98 (m, 12H), 1.19−1.68 (m, 6H), 1.71−2.30 (m, 4H), 2.56−2.96 (m, 3H), 3.15−3.40 (m, 1H), 4.16 (dd, *J* = 7.8, 14.2 Hz, 1H), 6.70−7.76 (m, 7H), 8.02 (d, *J* = 7.9 Hz, 1H), 8.25 (br s, 3H); ^{13}C NMR (50 MHz, DMSO-d_6/2% TFA) δ 21.6, 22.3, 23.0, 23.2, 24.4, 25.3, 29.7 (d, $^1J_{PC}$ = 92.8 Hz), 29.9, 31.8, 31.9, 38.1, 43.4, 43.6, 48.9 (d, $^1J_{PC}$ = 94.0 Hz), 51.4, 126.4, 128.5, 128.7, 141.0, 174.2, 174.3, 174.7; ^{31}P NMR (81 MHz, DMSO-d_6/2% TFA) δ 42.0. HRMS (*m*/*z*): $[M - H]^-$ calcd for $C_{22}H_{37}N_3O_4P^-$, 438.2527; found, 438.2524.

((1*R*)-1-Amino-3-phenylpropyl){(2′*S*)-2′-[((2″*S*)-1″-amino-1″-oxo-3″-phenylpropan-2″-yl)carbamoyl]-4′-methylpentyl}-phosphinic Acid (10c). Coupling of **4** with HBr·H-(L)Phe-NH_2 (**5c**) according to general procedure D and subsequent deprotection according to general procedure C afforded compound **6c** as a white solid (yield for two steps: 32%). ^{1}H NMR (200 MHz, DMSO-d_6/2% TFA) δ 0.59−0.85 (m, 6H), 1.10−1.41 (m, 3H), 1.57−2.20 (m, 4H),

DOI: 10.1021/acs.jmedchem.6b01031
J. Med. Chem. XXXX, XXX, XXX−XXX

2.55−2.94 (m, 4H), 2.97−3.36 (m, 2H), 4.29−4.51 (m, 1H), 6.97−7.76 (m, 12H), 8.10 (d, J = 7.4 Hz, 1H), 8.25 (br s, 3H); ^{13}C NMR (50 MHz, DMSO-d_6/2% TFA) δ 22.1, 23.0, 25.0, 29.6, 29.6 (d, $^1J_{PC}$ = 95.2 Hz), 31.5, 31.6, 32.6, 37.1, 42.8, 43.0, 48.5 (d, $^1J_{PC}$ = 95.0 Hz), 54.1, 126.2, 128.1, 128.3, 128.6, 129.2, 138.4, 140.8, 173.1, 173.8, 173.9; ^{31}P NMR (81 MHz, DMSO-d_6) δ 41.7. HRMS (m/z): [M − H]$^-$ calcd for $C_{25}H_{35}N_3O_4P^-$, 472.2371; found, 472.2366.

((1*R*)-1-Amino-3-phenylpropyl)[(2′*S*)-2′-((2″*S*)-2″-carbamoylpyrrolidine-1″-carbonyl)-4′-methylpentyl]phosphinic Acid (6d). Coupling of **4** with H-(L)Pro-NH$_2$ (**5d**) according to general procedure D and subsequent deprotection according to general procedure C afforded compound **6d** as a white solid (yield for two steps: 41%). ^{1}H NMR (200 MHz, DMSO-d_6/2% TFA) δ 0.84 (t, J = 6.3 Hz, 6H), 1.01−2.27 (m, 11H), 2.53−2.99 (m, 3H), 3.02−3.27 (m, 1H), 3.31−3.79 (m, 2H), 4.05−4.26 (m, 0.75H, major rotamer), 4.26−4.37 (m, 0.25H, minor rotamer), 6.73−7.86 (m, 7H), 8.22 (br s, 4H); ^{13}C NMR (50 MHz, DMSO-d_6/2% TFA, signals for major rotamer) δ 22.4, 23.0, 24.5, 24.8, 29.3 (d, $^1J_{PC}$ = 93.4 Hz), 29.4, 29.6, 31.5, 31.7, 34. 8, 42.7, 42.9, 47.1, 48.7 (d, $^1J_{PC}$ = 93.3 Hz), 59.5, 126.2, 128.3, 128.6, 140.9, 173.2, 173.3, 173.6; ^{31}P NMR (81 MHz, DMSO-d_6/2% TFA) δ 40.9 (minor), 41.2 (major), 42.0 (minor). HRMS (m/z): [M − H]$^-$ calcd for $C_{21}H_{33}N_3O_4P^-$, 422.2214; found, 422.2209.

((1*R*)-1-Amino-3-phenylpropyl)((2′*S*)-2′-{[(2″*S*)-1″-amino-3″-(1*H*-indol-3-yl)-1″-oxopropan-2″-yl]carbamoyl}-4′-methylpentyl)phosphinic Acid (6e). Coupling of **4** with H-(L)Trp-NH$_2$ (**5e**) according to general procedure D and subsequent deprotection according to general procedure C afforded compound **6e** as a white solid (yield for two steps: 32%). ^{1}H NMR (200 MHz, DMSO-d_6/2% TFA) δ 0.74 (dd, J = 4.3, 15.1 Hz, 6H), 1.14−1.50 (m, 3H), 1.68−2.26 (m, 4H), 2.53−2.91 (m, 3H), 2.92−3.39 (m, 3H), 4.44 (dd, J = 6.5, 12.9 Hz, 1H), 6.83−7.63 (m, 13H), 8.08 (d, J = 7.7 Hz, 1H), 8.24 (br s, 3H); ^{13}C NMR (50 MHz, DMSO-d_6/2% TFA) δ 22.2, 22.8, 25.1, 27.4, 29.7 (d, $^1J_{PC}$ = 92.4 Hz), 29.7, 31.5, 31.7, 38.0, 38.0, 43.1, 43.2, 48.5, 48.7 (d, $^1J_{PC}$ = 93.1 Hz), 53.8, 110.6, 111.4, 118.3, 118.6, 120.9, 123.6, 126.3, 127.5, 128.4, 128.6, 136.2, 140.9, 173.6, 174.0, 174.1; ^{31}P NMR (81 MHz, DMSO-d_6/2% TFA) δ 41.9. HRMS (m/z): [M − H]$^-$ calcd for $C_{27}H_{36}N_4O_4P^-$, 511.2480; found, 511.2462.

((1*R*)-1-Amino-3-phenylpropyl)((2′*S*)-2′-{[(2″*S*)-1″-amino-3″-(4-hydroxyphenyl)-1″-oxopropan-2″-yl]carbamoyl}-4′-methylpentyl)phosphinic Acid (6f). Coupling of **4** with H-(L)Tyr(*t*-Bu)-NH$_2$ (**5f**) according to general procedure D and subsequent deprotection according to general procedure C afforded compound **6f** as a white solid (yield for two steps: 55%). ^{1}H NMR (200 MHz, DMSO-d_6/2% TFA) δ 0.76 (dd, J = 4.8, 12.4 Hz, 6H), 1.14−1.48 (m, 3H), 1.67−2.24 (m, 4H), 2.55−3.03 (m, 5H), 3.08−3.32 (m, 1H), 4.31 (dd, J = 8.2, 13.6 Hz, 1H), 6.62 (d, J = 8.2 Hz, 2H), 6.90 (d, J = 8.2 Hz, 2H), 7.09−7.62 (m, 7H), 8.02 (d, J = 7.9 Hz, 1H), 8.23 (br s, 3H); ^{13}C NMR (50 MHz, DMSO-d_6/2% TFA) δ 22.2, 23.1, 25.2, 29.8 (d, $^1J_{PC}$ = 91.7 Hz), 29.9, 31.7, 31.8, 36.5, 43.2, 43.4, 48.8 (d, $^1J_{PC}$ = 94.2 Hz), 54.7, 115.1, 126.4, 128.5, 128.7, 130.2, 141.0, 156.0, 173.6, 174.0, 174.2; ^{31}P NMR (81 MHz, DMSO-d_6/2% TFA) δ 41.3. HRMS (m/z): [M − H]$^-$ calcd for $C_{25}H_{35}N_3O_5P^-$, 488.2320; found, 488.2322.

((1*R*)-1-Amino-3-phenylpropyl){(2′*S*)-2′-[((2″*S*)-1″-amino-3″-hydroxy-1″-oxopropan-2″-yl)carbamoyl]-4′-methylpentyl}-phosphinic Acid (6g). Coupling of **4** with H-(L)Ser(TBS)-NH$_2$ (**5g**) according to general procedure D and subsequent deprotection according to general procedure C afforded compound **6g** as a white solid (yield for two steps: 43%). ^{1}H NMR (200 MHz, DMSO-d_6/2% TFA) δ 0.83 (dd, J = 5.4, 11.9 Hz, 6H), 1.06−1.32 (m, 1H), 1.33−1.59 (m, 2H), 1.67−2.26 (m, 4H), 2.56−2.94 (m, 3H), 3.19−3.43 (m, 1H), 3.44−3.78 (m, 2H), 4.05−4.39 (m, 1H), 6.94−7.59 (m, 7H), 7.96 (d, J = 7.7 Hz, 1H), 8.24 (br s, 3H); ^{13}C NMR (50 MHz, DMSO-d_6/2% TFA) δ 22.4, 23.1, 25.4, 29.9, 30.3 (d, $^1J_{PC}$ = 92.0 Hz), 31.7, 31.9, 37.7, 37.8, 43.4, 43.7, 48.5 (d, $^1J_{PC}$ = 95.5 Hz), 55.6, 62.3, 126.5, 128.6, 128.8, 141.1, 172.3, 174.2, 174.3; ^{31}P NMR (81 MHz, DMSO-d_6/2% TFA) δ 41.6. HRMS (m/z): [M − H]$^-$ calcd for $C_{19}H_{31}N_3O_5P^-$, 412.2007; found, 412.2005.

((1*R*)-1-Amino-3-phenylpropyl){(2′*S*)-2′-[((2″*S*)-1″,6″-diamino-1″-oxohexan-2″-yl)carbamoyl]-4′-methylpentyl}-phosphinic Acid (6h). Coupling of **4** with H-(L)Lys(Boc)-NH$_2$ (**5h**) according to general procedure D and subsequent deprotection according to general procedure C afforded compound **6h** as a white solid (yield for two steps: 56%). ^{1}H NMR (200 MHz, DMSO-d_6/2% TFA) δ 0.84 (dd, J = 6.0, 11.4 Hz, 6H), 1.15−2.30 (m, 13H), 2.58−2.94 (m, 5H), 3.14−3.41 (m, 1H), 3.99−4.24 (m, 1H), 6.86−7.51 (m, 7H), 7.66 (br s, 2H), 8.01 (d, J = 7.7 Hz, 1H), 8.25 (br s, 3H); ^{13}C NMR (50 MHz, DMSO-d_6/2% TFA) δ 22.7, 22.8, 23.1, 25.6, 27.0, 29.9 (d, $^1J_{PC}$ = 93.3 Hz), 30.1, 31.5, 32.1, 32.3, 44.0, 44.2, 49.3 (d, $^1J_{PC}$ = 93.3 Hz), 53.0, 126.8, 128.9, 129.1, 141.3, 174.9, 175.0, 175.1; ^{31}P NMR (81 MHz, DMSO-d_6/2% TFA) δ 40.8. HRMS (m/z): [M − H]$^-$ calcd for $C_{22}H_{38}N_4O_4P^-$, 453.2636; found, 453.2634.

((1*R*)-1-Amino-3-phenylpropyl)((2′*S*)-2′-[((2″*S*)-1″-amino-3″-(1*H*-imidazol-4-yl)-1″-oxopropan-2″-yl]carbamoyl}-4′-methylpentyl)phosphinic Acid (6i). Coupling of **4** with H-(L)His(Boc)-NH$_2$ (**5i**) according to general procedure D and subsequent deprotection according to general procedure C afforded compound **6i** as a white solid (yield for two steps: 10%). ^{1}H NMR (200 MHz, DMSO-d_6/2% TFA) δ 0.53−0.94 (m, 6H), 0.99−1.61 (m, 3H), 1.66−2.28 (m, 4H), 2.55−2.92 (m, 4H), 2.94−3.15 (m, 1H), 3.16−3.50 (m, 1H), 4.39−4.61 (m, 1H), 6.98−7.77 (m, 9H), 8.10 (d, J = 7.8 Hz, 1H), 8.27 (br s, 3H), 8.89 (br s, 1H); ^{31}P NMR (81 MHz, DMSO-d_6/2% TFA) δ 41.9, (41.7: minor rotamer). HRMS (m/z): [M − H]$^-$ calcd for $C_{22}H_{33}N_5O_4P^-$, 462.2276; found, 462.2274.

(4″*S*)-5″-Amino-4″-((2′*S*)-2′-{[((1*R*)-1-amino-3-phenylpropyl)(hydroxy)phosphoryl]methyl}-4′-methylpentanamido)-5″-oxopentanoic Acid (6j). Coupling of **4** with HCl·H-(L)Glu(*t*-Bu)-NH$_2$ (**5j**) according to general procedure D and subsequent deprotection according to general procedure C afforded compound **6j** as a white solid (yield for two steps: 52%). ^{1}H NMR (200 MHz, DMSO-d_6/2% TFA) δ 0.84 (dd, J = 5.5, 11.2 Hz, 6H), 1.13−1.38 (m, 1H), 1.38−1.60 (m, 2H), 1.66−2.33 (m, 8H), 2.60−2.94 (m, 3H), 3.12−3.38 (m, 1H), 4.01−4.26 (m, 1H), 6.82−7.53 (m, 7H), 8.09 (d, J = 7.6 Hz, 1H), 8.23 (br s, 3H); ^{13}C NMR (50 MHz, DMSO-d_6/2% TFA) δ 22.4, 23.0, 25.2, 27.2, 29.7 (d, $^1J_{PC}$ = 94.7 Hz), 29.8, 30.6, 31.6, 31.8, 37.8, 37.9, 43.3, 43.6, 48.7 (d, $^1J_{PC}$ = 94.5 Hz), 52.2, 126.3, 128.5, 128.7, 141.0, 173.5, 174.2, 174.4; ^{31}P NMR (81 MHz, DMSO-d_6/2% TFA) δ 41.2. HRMS (m/z): [M − H]$^-$ calcd for $C_{21}H_{33}N_3O_6P^-$, 454.2112; found, 454.2110.

((1*R*)-1-Amino-3-phenylpropyl){(2′*S*)-2′-[((2″*R*)-1″-amino-1″-oxo-3″-phenylpropan-2″-yl)carbamoyl]-4′-methylpentyl}-phosphinic Acid (6k). Coupling of **4** with HBr·H-(D)Phe-NH$_2$ (**5k**) according to general procedure D and subsequent deprotection according to general procedure C afforded compound **6k** as a white solid (yield for two steps: 31%). ^{1}H NMR (200 MHz, DMSO-d_6/2% TFA) δ 0.61 (dd, J = 3.6, 16.4 Hz, 6H), 0.81−1.36 (m, 3H), 1.56−2.21 (m, 4H), 2.42−2.94 (m, 4H), 3.11−3.39 (m, 2H), 4.25−4.56 (m, 1H), 6.91−7.41 (m, 12H), 8.21 (br s, 3H), 8.35 (d, J = 8.0 Hz, 1H); ^{13}C NMR (50 MHz, DMSO-d_6/2% TFA) δ 22.2, 23.3, 24.7, 29.7, 30.0 (d, $^1J_{PC}$ = 90.1 Hz), 31.7, 31.9, 37.1, 37.6, 44.0, 44.3, 49.0 (d, $^1J_{PC}$ = 95.0 Hz), 54.6, 126.4, 126.5, 128.3, 128.6, 129.4, 138.9, 141.0, 174.2, 174.4, 174.5; ^{31}P NMR (81 MHz, DMSO-d_6/2% TFA) δ 41.6. HRMS (m/z): [M − H]$^-$ calcd for $C_{25}H_{35}N_3O_4P^-$, 472.2371; found, 472.2357.

2′-{[((1*R*)-1-{[(*tert*-Butoxy)carbonyl]amino}-3-phenylpropyl)(hydroxy)phosphoryl]methyl}pent-4′-ynoic Acid (8). Addition of phosphinic acid **7** (1.0 g, 3.3 mmol) to ethyl 2-methylenepent-4-ynoate[25] (0.59 g, 4.3 mmol) according to general procedure A and subsequent saponification according to general procedure B afforded compound **8** as a mixture of two diastereoisomers *RS*/*RR* = 67:33 (1.34 g, 99% starting from **7**). ^{1}H NMR (500 MHz, DMSO-d_6) δ [1.36 (s, minor rotamer) + 1.40 (s), 9H], 1.66−1.88 (m, 2H), 1.88−2.13 (m, 2H), 2.44−2.65 (m, 3H), 2.66−2.90 (m, 3H), 3.42−3.71 (m, 1H), [6.65 (d, J = 9.8 Hz, minor rotamer) + 6.69 (d, J = 9.1 Hz), 1H], 7.05−7.42 (m, 5H); ^{13}C NMR (50 MHz, DMSO-d_6, signals for major rotamer) δ 21.5, 21.6, 26.5 ($^1J_{PC}$ = 89.0 Hz), 28.3, 29.0, 31.7, 31.9, 37.6, 49.2 ($^1J_{PC}$ = 107 Hz), 72.9, 78.4, 81.4, 126.0, 128.4, 128.6, 141.4, 155.7, 155.8, 174.2, 174.5; ^{31}P NMR (81 MHz, DMSO-d_6) δ 47.5, 47.1. ES-MS m/z: calcd for [$C_{20}H_{28}NO_6P$ − H]$^-$ 408.2; found, 408.3. HRMS (m/z): [M + H]$^+$ calcd for $C_{20}H_{29}NO_6P^+$, 410.1727; found, 410.1733.

DOI: 10.1021/acs.jmedchem.6b01031
J. Med. Chem. XXXX, XXX, XXX−XXX

((1*R*)-1-{[(*tert*-Butoxy)carbonyl]amino}-3-phenylpropyl)-{(2′*S*)-2′-[((2″*S*)-1″-amino-1″-oxo-3″-phenylpropan-2″-yl)-carbamoyl]pent-4′-yn-1′-yl}phosphinic Acid (9). Phosphinic tripeptide **9** was isolated as a white solid after coupling of **8** (1.3 g, 3.2 mmol) with HBr·H-(L)Phe-NH_2 (**5c**) according to general procedure D and recrystallization of the crude product by AcOEt (0.73 g, 41% starting from **8**). ^{1}H NMR (500 MHz, DMSO-d_6) δ [1.35 (s, minor rotamer) + 1.42 (s), 9H], 1.70−1.84 (m, 3H), 1.88−2.00 (m, 1H), 2.21 (dd, J = 6.3, 16.5, 1H), 2.33 (dd, J = 6.3, 16.7, 1H), 2.43−2.49 (m, 1H), 2.65−2.77 (m, 2H), 2.74 (s, 1H), 2.83 (dd, J = 9.4, 13.7, 1H), 3.08 (dd, J = 4.7, 13.7, 1H), 3.58 (dd, J = 9.2, 20.5, 1H), 4.33 (dt, J = 5.2, 8.7, 1H), 7.02 (br s, 1H), 7.07 (d, J = 9.4 Hz, 1H), 7.11−7.33 (m, 10H), 7.55 (br s, 1H), 8.07 (d, J = 7.5 Hz, 1H); ^{13}C NMR (125 MHz, DMSO-d_6, signals for major rotamer) δ 22.2, 22.3, 27.2 ($^1J_{PC}$ = 87.4 Hz), 28.3, 29.2, 31.7, 31.8, 37.0, 38.8, 49.6 ($^1J_{PC}$ = 106.2 Hz), 54.1, 72.5, 78.3, 81.9, 125.9, 126.1, 128.0, 128.3, 128.5, 129.2, 138.3, 141.4, 155.7, 172.1, 172.1, 172.9; ^{31}P NMR (81 MHz, DMSO-d_6) δ 47.3, (47.0: minor rotamer). ES-MS m/z: calcd for $[C_{29}H_{38}N_3O_6P - H]^-$ 554.3; found, 554.3. HRMS (m/z): $[M + H]^+$ calcd for $C_{29}H_{39}N_3O_6P^+$, 556.2571; found, 556.2566.

((1*R*)-1-Amino-3-phenylpropyl){(2′*S*)-3′-[((2″*S*)-1″-amino-1″-oxo-3″-phenylpropan-2″-yl)amino]-3′-oxo-2′-[(3-phenylisoxazol-5-yl)methyl]propyl}phosphinic Acid (13a). 1,3-DCR between **9** and oxime **11a** according to general procedure E (no repetition was necessary for completion) and subsequent deprotection according to general procedure C afforded compound **13a** as a white solid (yield for two steps: 80%). ^{1}H NMR (500 MHz, DMSO-d_6/3% TFA) δ 1.81−1.93 (m, 2H), 1.96−2.10 (m, 2H), 2.60−2.70 (m, 1H), 2.76−2.90 (m, 2H), 3.00−3.09 (m, 2H), 3.09−3.15 (m, 1H), 3.19 (d, J = 4.7, 14.8 Hz, 1H), 3.22−3.30 (m, 1H), 4.43 (dt, J = 5.7, 8.7 Hz, 1H), 6.70 (s, 1H), 7.01−7.85 (m, 17H), 8.28 (br s, 3H), 8.43 (d, J = 8.2 Hz, 1H); ^{13}C NMR (125 MHz, DMSO-d_6/2% TFA) δ 29.3 (d, $^1J_{PC}$ = 92.3 Hz), 29.7, 31.6, 31.7, 37.5, 37.9, 48.7 (d, $^1J_{PC}$ = 94.9 Hz), 54.2, 100.4, 126.2, 126.3, 126.6, 128.1, 128.3, 128.5, 128.9, 129.1, 129.2, 130.1, 138.1, 140.9, 161.9, 171.4, 172.3, 172.4, 173.0; ^{31}P NMR (81 MHz, DMSO-d_6/3% TFA) δ 40.5. HRMS (m/z): $[M - H]^-$ calcd for $C_{31}H_{34}N_4O_5P^-$, 573.2272; found, 573.2216.

((1*R*)-1-Amino-3-phenylpropyl){(2′*S*)-3′-[((2″*S*)-1″-amino-1″-oxo-3″-phenylpropan-2″-yl)amino]-2′-{[3-(2-methoxyphenyl)-isoxazol-5-yl]methyl}-3′-oxopropyl}phosphinic Acid (13b). 1,3-DCR between **9** and oxime **11b** according to general procedure E (no repetition was necessary for completion) and subsequent deprotection according to general procedure C afforded compound **13b** as a white solid (yield for two steps: 85%). ^{1}H NMR (200 MHz, DMSO-d_6 + $CDCl_3$/3% TFA) δ 1.55−2.20 (m, 4H), 2.54−3.34 (m, 8H), 3.83 (s, 3H), 4.26−4.56 (m, 1H), 6.58 (s, 1H), 6.84−7.79 (m, 16H), 8.02−8.53 (m, 4H); ^{13}C NMR (50 MHz, DMSO-d_6 + $CDCl_3$/3% TFA) δ 29.1 (d, $^1J_{PC}$ = 92.5 Hz), 29.9, 31.7, 31.9, 37.6, 38.0, 48.7 (d, $^1J_{PC}$ = 96.1 Hz), 54.3, 55.7, 103.5, 112.1, 117.5, 120.8, 126.3, 128.1, 128.4, 128.6, 128.9, 129.4, 131.5, 138.2, 140.9, 157.0, 159.6, 170.1, 172.3, 172.5, 173.0; ^{31}P NMR (81 MHz, DMSO-d_6/3% TFA) δ 40.1. HRMS (m/z): $[M - H]^-$ calcd for $C_{32}H_{36}N_4O_6P^-$, 603.2378; found, 603.2351.

((1*R*)-1-Amino-3-phenylpropyl){(2′*S*)-3′-[((2″*S*)-1″-amino-1″-oxo-3″-phenylpropan-2″-yl)amino]-2′-{[3-(3-methoxyphenyl)-isoxazol-5-yl]methyl}-3′-oxopropyl}phosphinic Acid (13c). 1,3-DCR between **9** and oxime **11c** according to general procedure E (one repetition was necessary for completion) and subsequent deprotection according to general procedure C afforded compound **13c** as a white solid (yield for two steps: 75%). ^{1}H NMR (200 MHz, DMSO-d_6/5% TFA) δ 1.66−2.14 (m, 4H), 2.52−2.94 (m, 3H), 2.95−3.38 (m, 5H), 3.80 (s, 3H), 4.33−4.56 (m, 1H), 6.74 (s, 1H), 6.84−7.68 (m, 16H), 8.30 (br s, 3H), 8.48 (d, J = 7.4 Hz, 1H); ^{13}C NMR (50 MHz, DMSO-d_6/5% TFA) δ 29.4 (d, $^1J_{PC}$ = 93.9 Hz), 29.9, 31.7, 31.9, 37.0, 37.7, 38.0, 48.9 (d, $^1J_{PC}$ = 93.9 Hz), 54.4, 55.5, 100.7, 112.1, 116.2, 119.1, 126.4, 128.3, 128.4, 128.5, 128.7, 129.4, 130.1, 130.5, 131.5, 137.7, 138.3, 141.0, 159.9, 162.0, 171.6, 172.5, 172.7, 173.1, 173.2; ^{31}P NMR (81 MHz, DMSO-d_6/5% TFA) δ 40.5. HRMS (m/z): $[M - H]^-$ calcd for $C_{32}H_{36}N_4O_6P^-$, 603.2378; found, 603.2379.

((1*R*)-1-Amino-3-phenylpropyl){(2′*S*)-3′-[((2″*S*)-1″-amino-1″-oxo-3″-phenylpropan-2″-yl)amino]-2′-{[3-(4-methoxyphenyl)-isoxazol-5-yl]methyl}-3′-oxopropyl}phosphinic Acid (13d). 1,3-DCR between **9** and oxime **11d** according to general procedure E (2 repetitions were necessary for completion) and subsequent deprotection according to general procedure C afforded compound **13d** as a white solid (yield for two steps: 76%). ^{1}H NMR (200 MHz, DMSO-d_6/5% TFA) δ 1.70−2.21 (m, 4H), 2.35−2.94 (m, 3H), 2.94−3.40 (m, 5H), 3.79 (s, 3H), 4.33−4.55 (m, 1H), 6.63 (s, 1H), 6.82−7.85 (m, 16H), 8.27 (br s, 3H), 8.47 (d, J = 7.7 Hz, 1H); ^{13}C NMR (50 MHz, DMSO-d_6/5% TFA) δ 29.3 (d, $^1J_{PC}$ = 94.6 Hz), 29.9, 31.7, 31.9, 37.7, 38.1, 48.8 (d, $^1J_{PC}$ = 95.6 Hz), 54.4, 55.4, 100.4, 114.7, 121.4, 126.4, 128.3, 128.5, 128.8, 129.5, 138.3, 141.0, 160.9, 161.7, 171.1, 172.4, 172.6, 173.2; ^{31}P NMR (81 MHz, DMSO-d_6/5% TFA) δ 41.2. HRMS (m/z): $[M - H]^-$ calcd for $C_{32}H_{36}N_4O_6P^-$, 603.2378; found, 603.2382.

((1*R*)-1-Amino-3-phenylpropyl){(2′*S*)-3′-[((2″*S*)-1″-amino-1″-oxo-3″-phenylpropan-2″-yl)amino]-2′-{[3-(2-chlorophenyl)-isoxazol-5-yl]methyl}-3′-oxopropyl}phosphinic Acid (13e). 1,3-DCR between **9** and oxime **11e** according to general procedure E (no repetition was necessary for completion) and subsequent deprotection according to general procedure C afforded compound **9e** as a white solid (yield for two steps: 73%). ^{1}H NMR (200 MHz, DMSO-d_6/4% TFA) δ 1.69−2.21 (m, 4H), 2.53−2.93 (m, 3H), 2.93−3.36 (m, 5H), 4.29−4.52 (m, 1H), 6.58 (s, 1H), 6.81−7.71 (m, 16H), 8.28 (br s, 3H), 8.40 (d, J = 8.2 Hz, 1H); ^{13}C NMR (50 MHz, DMSO-d_6/4% TFA) δ 29.8 (d, $^1J_{PC}$ = 92.6 Hz), 29.9, 31.6, 31.8, 37.0, 37.7, 38.0, 48.7 (d, $^1J_{PC}$ = 94.7 Hz), 54.2, 103.4, 126.4, 127.8, 128.2, 128.3, 128.4, 128.7, 129.4, 130.6, 131.2, 131.6, 132.0, 138.2, 140.9, 160.7, 170.9, 172.2, 172.4, 172.9; ^{31}P NMR (81 MHz, DMSO-d_6/4% TFA) δ 40.8. HRMS (m/z): $[M - H]^-$ calcd for $C_{31}H_{33}ClN_4O_5P^-$, 607.1883; found, 607.1876.

((1*R*)-1-Amino-3-phenylpropyl){(2′*S*)-3′-[((2″*S*)-1″-amino-1″-oxo-3″-phenylpropan-2″-yl)amino]-2′-{[3-(3-chlorophenyl)-isoxazol-5-yl]methyl}-3′-oxopropyl}phosphinic Acid (13f). 1,3-DCR between **9** and oxime **11f** according to general procedure E (5 repetitions were necessary for completion) and subsequent deprotection according to general procedure C afforded compound **13f** as a white solid (yield for two steps: 67%). ^{1}H NMR (500 MHz, DMSO-d_6/3% TFA) δ 1.75−1.95 (m, 2H), 1.96−2.11 (m, 2H), 2.57−2.72 (m, 1H), 2.75−2.91 (m, 2H), 2.95−3.40 (m, 5H), 4.32−4.49 (m, 1H), 6.76 (s, 1H), 7.00−7.93 (m, 16H), 8.30 (br s, 3H), 8.45 (d, J = 7.3 Hz, 1H); ^{13}C NMR (50 MHz, DMSO-d_6/3% TFA) δ 29.3 (d, $^1J_{PC}$ = 93.1 Hz), 29.8, 31.5, 31.7, 37.5, 37.8, 37.9, 48.7 (d, $^1J_{PC}$ = 94.2 Hz), 54.2, 100.5, 125.2, 126.2, 128.1, 128.3, 128.5, 129.2, 130.0, 130.8, 131.1, 133.9, 138.1, 140.9, 160.8, 171.8, 172.2, 172.4, 173.0; ^{31}P NMR (81 MHz, DMSO-d_6/3% TFA) δ 39.8. HRMS (m/z): $[M - H]^-$ calcd for $C_{31}H_{33}ClN_4O_5P^-$, 607.1883; found, 607.1880.

((1*R*)-1-Amino-3-phenylpropyl){(2′*S*)-3′-[((2″*S*)-1″-amino-1″-oxo-3″-phenylpropan-2″-yl)amino]-2′-{[3-(4-chlorophenyl)-isoxazol-5-yl]methyl}-3′-oxopropyl}phosphinic Acid (13g). 1,3-DCR between **9** and oxime **11g** according to general procedure E (4 repetitions were necessary for completion) and subsequent deprotection according to general procedure C afforded compound **13g** as a white solid (yield for two steps: 67%). ^{1}H NMR (200 MHz, DMSO-d_6/5% TFA) δ 1.69−2.18 (m, 4H), 2.57−2.95 (m, 3H), 2.95−3.37 (m, 5H), 4.28−4.52 (m, 1H), 6.71 (s, 1H), 6.88−7.91 (m, 16H), 8.30 (br s, 3H), 8.47 (d, J = 7.8 Hz, 1H); ^{13}C NMR (50 MHz, DMSO-d_6/5% TFA) δ 29.4 (d, $^1J_{PC}$ = 93.5 Hz), 30.0, 31.8, 32.0, 37.1, 37.7, 48.9 (d, $^1J_{PC}$ = 96.2 Hz), 54.5, 100.7, 126.4, 126.5, 128.0, 128.3, 128.6, 128.8, 129.5, 135.1, 138.4, 141.1, 161.2, 172.0, 172.5, 172.7, 173.4; ^{31}P NMR (81 MHz, DMSO-d_6/5% TFA) δ 40.8. HRMS (m/z): $[M - H]^-$ calcd for $C_{31}H_{33}ClN_4O_5P^-$, 607.1883; found, 607.1863.

((1*R*)-1-Amino-3-phenylpropyl){(2′*S*)-3′-[((2″*S*)-1″-amino-1″-oxo-3″-phenylpropan-2″-yl)amino]-2′-{[3-(2-hydroxyphenyl)-isoxazol-5-yl]methyl}-3′-oxopropyl}phosphinic Acid (13h). 1,3-DCR between **9** and oxime **11h** was performed according to general procedure E (no repetition was necessary for completion). The product was dissolved in DMF/H_2O 10:1 (2 mL/mmol) and Cs_2CO_3 (2 equiv) was added. After stirring at rt overnight, the mixture was acidified with 1 M HCl to pH 1, extracted with AcOEt (× 3). After concentration in vacuo of the organic layer, the residue was subjected to deprotection according to general procedure C, affording

DOI: 10.1021/acs.jmedchem.6b01031
J. Med. Chem. XXXX, XXX, XXX−XXX

compound **13h** as a white solid (yield for three steps: 51%). ^{1}H NMR (200 MHz, DMSO-d_6/2% TFA) δ 1.64−2.20 (m, 4H), 2.36−2.93 (m, 3H), 2.94−3.42 (m, 5H), 4.28−4.50 (m, 1H), 6.75 (s, 1H), 6.62−7.56 (m, 16H), 7.69 (d, J = 7.3 Hz, 1H), 8.29 (br s, 3H); ^{13}C NMR (50 MHz, DMSO-d_6/2% TFA) δ 29.2 (d, $^1J_{PC}$ = 91.2 Hz), 29.9, 31.6, 31.8, 37.5, 48.7 (d, $^1J_{PC}$ = 94.3 Hz), 54.3, 102.9, 115.2, 116.8, 119.5, 126.3, 128.2, 128.4, 128.6, 129.3, 131.3, 138.2, 141.0, 155.7, 160.4, 170.1, 172.4, 172.5, 172.9; ^{31}P NMR (81 MHz, DMSO-d_6/2% TFA) δ 40.1. HRMS (m/z): [M − H]$^-$ calcd for $C_{31}H_{34}N_4O_6P^-$, 589.2221; found, 589.2219.

((1*R*)-1-Amino-3-phenylpropyl){(2′*S*)-3′-[((2″*S*)-1″-amino-1″-oxo-3″-phenylpropan-2″-yl)amino]-2′-{[3-(4-hydroxyphenyl)-isoxazol-5-yl]methyl}-3′-oxopropyl}phosphinic Acid (13i). 1,3-DCR between **9** and oxime **11i** was performed according to general procedure E (2 repetitions were necessary for completion). The product was treated with Cs_2CO_3 as described above and subjected to deprotection according to general procedure C, affording compound **13i** as a white solid (yield for three steps: 61%). ^{1}H NMR (500 MHz, DMSO-d_6/3.5% TFA) δ 1.76−1.96 (m, 2H), 1.98−2.17 (m, 2H), 2.59−2.73 (m, 1H), 2.73−2.95 (m, 2H), 2.95−3.68 (m, 5H), 4.35−4.54 (m, 1H), 6.54 (s, 1H), 6.78−7.69 (m, 16H), 8.30 (br s, 3H), 8.44 (d, J = 7.8 Hz, 1H); ^{13}C NMR (50 MHz, DMSO-d_6/3.5% TFA) δ 29.5 (d, $^1J_{PC}$ = 92.0 Hz), 30.1, 31.9, 32.1, 37.8, 49.0 (d, $^1J_{PC}$ = 95.8 Hz), 54.6, 100.3, 116.2, 119.9, 126.5, 126.6, 128.4, 128.6, 128.8, 129.6, 138.4, 141.2, 159.5, 162.1, 171.1, 172.7, 172.8, 173.4; ^{31}P NMR (81 MHz, DMSO-d_6/23.5% TFA) δ 40.1. HRMS (m/z): [M − H]$^-$ calcd for $C_{31}H_{34}N_4O_6P^-$, 589.2221; found, 589.2233.

((1*R*)-1-Amino-3-phenylpropyl){(2′*S*)-2′-[((2″*S*)-1″-amino-1″-oxo-3″-phenylpropan-2″-yl)carbamoyl]pent-4′-yn-1′-yl}-phosphinic Acid (14). Phosphinic tripeptide **9** (24 mg, 43 μmol) was subjected to deprotection according to general procedure C, affording compound **14** as a white solid (17 mg, 87%). ^{1}H NMR (250 MHz, DMSO-d_6/5% TFA) δ 1.76−2.19 (m, 4H), 2.35−2.70 (m, 3H), 2.72−2.91 (m, 4H), 3.03 (dd, J = 5.2, 13.7, 1H), 3.11−3.26 (m, 1H), 4.38 (dd, J = 8.1, 13.5, 1H), 7.01−7.45 (m, 12H), 8.14−8.33 (m, 4H); ^{13}C NMR (63 MHz, DMSO-d_6/5% TFA) δ 22.7, 22.9, 28.4 ($^1J_{PC}$ = 92.9 Hz), 29.7, 31.6, 31.7, 48.7 ($^1J_{PC}$ = 95.6 Hz), 54.4, 73.2, 81.8, 126.3, 128.2, 128.4, 128.7, 129.4, 138.2, 140.9, 155.7, 172.3, 172.4, 172.8; ^{31}P NMR (81 MHz, DMSO-d_6/5% TFA) δ 41.7. HRMS (m/z): [M − H]$^-$ calcd for $C_{24}H_{29}N_3O_4P^-$, 454.1901; found, 454.1893.

Ethyl 2-Methylene-4,4-diphenylbutanoate (15). A solution of DCC (1.18 g, 5.72 mmol) in dry CH_2Cl_2 (11 mL) was added to a solution of 2,2-diphenylacetic acid (1.0 g, 4.7 mmol), Meldrum's acid (0.75 g, 5.2 mmol), and DMAP (0.92 g, 7.5 mmol) in CH_2Cl_2 (22 mL) at 0 °C over a period of 1 h. After stirring at rt for 3 h, the reaction mixture was cooled at −10 °C overnight. The solid precipitate was removed by filtration through a Celite pad, and the filtrates were concentrated in vacuo. The residue was dissolved in AcOEt (20 mL) and washed with sat. $NaHSO_4$ (2 × 10 mL) and brine (10 mL). The organic phase was dried over Na_2SO_4 and evaporated in vacuo. The residue was dissolved in dry CH_2Cl_2 (15 mL), and AcOH (3.5 mL) was added at 0 °C. Then, $NaBH_4$ (0.60 g, 15.8 mmol) was added over a period of 2 h. After stirring at rt overnight, the reaction mixture was washed with H_2O (2 × 10 mL) and brine (10 mL) and the organic phase was dried over Na_2SO_4 and concentrated in vacuo. The residue was purified by column chromatography (PE 40−60 °C/AcOEt 3:7) to afford the alkylated Meldrum's derivative as a white solid (0.75 g, 49%): mp 145−147 °C; ^{1}H NMR (200 MHz, $CDCl_3$) δ 1.57 (s, 3H), 1.71 (s, 3H), 2.79 (dd, J = 6.0, 8.5 Hz, 2H), 3.28 (t, J = 6.0 Hz, 1H), 4.59 (t, J = 8.5 Hz, 1H), 7.12−7.41 (m, 10H); ^{13}C NMR (50 MHz, $CDCl_3$) δ 26.3, 28.7, 32.0, 44.4, 48.3, 105.1, 127.0, 128.1, 129.0, 143.0, 165.7. A solution of the above derivative (500 mg, 1.54 mmol) and Eschenmoser's salt (712 mg, 3.85 mmol) in THF/abs EtOH 1:3 (15 mL) was heated at 65 °C overnight, and then the mixture was cooled at rt, diluted with AcOEt (20 mL), and washed with 10% Na_2CO_3 (10 mL), H_2O (2 × 10 mL), and 2 M HCl (10 mL). The organic phase was dried over Na_2SO_4 and concentrated in vacuo. The residue was purified by column chromatography (PE 40−60 °C/AcOEt 9.5:0.5 → 2:1) to afford **15** as a light-yellow viscous oil (402 mg, 93%). ^{1}H NMR (200 MHz, $CDCl_3$) δ 1.33 (t, J = 7.1 Hz, 3H), 3.14 (dd, J = 0.7, 7.8 Hz, 2H), 4.23 (q, J = 7.1 Hz, 2H), 4.33 (t, J = 7.8 Hz, 1H), 5.36 (d, J = 1.2 Hz, 1H), 6.13 (d, J = 1.2 Hz, 1H), 7.11−7.41 (m, 10H); ^{13}C NMR (50 MHz, $CDCl_3$) δ 14.3, 38.1, 50.0, 60.7, 126.3, 127.0, 128.1, 128.5, 138.6, 144.1, 167.1. HRMS (m/z): [M + Na]$^+$ calcd for $C_{19}H_{20}NaO_2^+$, 303.1356; found, 303.1359.

[1,1′:3′,1″-Terphenyl]-5′-carbaldehyde (17a). A mixture of 3,5-dibromobenzaldehyde (0.60 g, 2.27 mmol), DME (24 mL), H_2O (5 mL), phenylboronic acid (0.75 g, 6.15 mmol), and Na_2CO_3 (0.96 g, 9.08 mmol) was degassed by applying three freeze−pump−thaw cycles. Then, $Pd(PPh_3)_4$ (262 mg, 0.227 mmol) was added, and the resulting suspension was heated at 90 °C overnight. The mixture was diluted with Et_2O (20 mL), and the organic phase was washed with H_2O (2 × 10 mL), dried over Na_2SO_4, and concentrated in vacuo. The residue was purified by column chromatography (PE 40−60 °C/AcOEt 9.8:0.2 → 0:1) to afford **17a** as a white solid (0.57 g, 98%). Mp 96−98 °C; ^{1}H NMR (200 MHz, $CDCl_3$) δ 7.39−7.59 (m, 6H), 7.62−7.76 (m, 4H), 8.07 (s, 3H), 10.13 (s, 1H); ^{13}C NMR (50 MHz, $CDCl_3$) δ 127.1, 127.2, 128.1, 129.0, 131.7, 137.4, 139.6, 142.6, 192.2. HRMS (m/z): [M + Na]$^+$ calcd for $C_{19}H_{14}NaO^+$, 281.0937; found, 281.0938.

3,3″-Dichloro-[1,1′:3′,1″-terphenyl]-5′-carbaldehyde (17b). 3,5-Dibromobenzaldehyde (0.75 g, 2.84 mmol) and boronic acid **16b** (1.60 g, 10.2 mmol) were converted to **17b** by following the same procedure as described for the synthesis of **17a**. Compound **17b** was obtained as a white solid (0.76 g, 82%). Mp 131−134 °C; ^{1}H NMR (200 MHz, $CDCl_3$) δ 7.31−7.69 (m, 8H), 7.92−8.15 (m, 3H), 10.16 (s, 1H); ^{13}C NMR (50 MHz, $CDCl_3$) δ 125.4, 127.3, 127.5, 128.3, 130.4, 131.4, 135.0, 137.6, 141.2, 141.5, 191.8.

5′-(Bromomethyl)-1,1′:3′,1″-terphenyl (18a). In an ice-cooled solution of aldehyde **17a** (504 mg, 1.95 mmol) in EtOH (20 mL), $NaBH_4$ (74 mg, 1.95 mmol) was slowly added. The mixture was stirred at rt during 1.5 h and then quenched with dilute HCl. The mixture was partitioned with Et_2O (30 mL) and H_2O (10 mL), and the aqueous phase was washed with Et_2O (3 × 10 mL). The combined organic layers were dried over Na_2SO_4 and concentrated in vacuo. The resulting white solid was dissolved in dry CH_2Cl_2 (10 mL), and PBr_3 (0.18 mL, 1.95 mmol) was added dropwise at 0 °C over a period of 5 min. After stirring at rt for 1 h, the organic phase was washed with H_2O (2 × 10 mL), dried over Na_2SO_4, and concentrated in vacuo. Compound **18a** was obtained as an off-white solid (0.57 g, 91%). Mp 92−94 °C; ^{1}H NMR (200 MHz, $CDCl_3$) δ 4.62 (s, 2H), 7.30−7.81 (m, 13H); ^{13}C NMR (50 MHz, $CDCl_3$) δ 33.6, 125.6, 126.4, 126.9, 127.4, 127.8, 129.9, 138.8, 140.6, 142.4, 142.5.

5′-(Bromomethyl)-3,3″-dichloro-1,1′:3′,1″-terphenyl (18b). Compound **17b** (0.77 g, 2.34 mmol) was converted to **18b** by following the same procedure as described for the synthesis of **18a**. White solid (0.74 g, 81%). Mp 96−100 °C; ^{1}H NMR (200 MHz, $CDCl_3$) δ 4.60 (s, 2H), 7.16−7.66 (m, 11H); ^{13}C NMR (50 MHz, $CDCl_3$) δ 33.1, 125.5, 126.1, 127.3, 127.5, 128.0, 130.3, 134.9, 139.3, 141.3, 142.1. ES-MS m/z: calcd for [$C_{19}H_{13}BrCl_2$ − H]$^-$ 391.0; found, 390.8.

Ethyl 2-([1,1′:3′,1″-Terphenyl]-5′-ylmethyl)acrylate (19a). A suspension of compound **18a** (0.58 g, 1.78 mmol), triethyl methanetricarboxylate (0.42 mL, 1.95 mmol), and K_2CO_3 (0.27 mg, 1.97 mmol) in DMF/toluene 1:1 (30 mL) was refluxed over a period of 1.5 h. Then, H_2O (50 mL) was added, the organic phase was separated, and the aqueous phase was extracted with AcOEt (2 × 15 mL). The combined organic layers were dried over Na_2SO_4, concentrated in vacuo, and the resulting orange oil was dissolved in EtOH (10 mL). A solution of KOH (1.1 g, 19 mmol) in EtOH (3 mL) was added at 0 °C, and the mixture was stirred at rt overnight. After evaporation of the volatiles, the residue was dissolved in H_2O (20 mL) and the aqueous solution was washed with Et_2O (3 × 5 mL), acidified to pH 1, and extracted with AcOEt (4 × 20 mL). The combined organic layers were dried over Na_2SO_4, concentrated in vacuo, and the resulting yellowish oil was dissolved in AcOEt (7 mL). After the addition of Et_2NH (0.24 mL, 2.35 mmol) and paraformaldehyde (86 mg, 2.88 mmol), the mixture was refluxed during 4 h. Then, the volatiles were evaporated, and the residue was dissolved in H_2O (30 mL), acidified to pH 1, and extracted with AcOEt (2 × 20 mL). The

DOI: 10.1021/acs.jmedchem.6b01031
J. Med. Chem. XXXX, XXX, XXX−XXX

combined organic layers were dried over Na_2SO_4 and concentrated in vacuo. The resulting crude acrylic acid (0.38 g, 1.22 mmol) was dissolved in dry CH_2Cl_2 (3 mL), and EtOH (0.14 mL, 2.4 mmol), DIPEA (0.28 mL, 1.6 mmol), EDC·HCl (307 mg, 1.6 mmol), and DMAP (15 mg, 0.12 mmol) were succesively added. The mixture was stirred overnight at rt, and then it was concentrated to dryness. The residue was dissolved in AcOEt (20 mL) and washed with H_2O (2 × 5 mL), 5% $NaHCO_3$ (2 × 5 mL), 1 M HCl (2 × 5 mL), and brine (5 mL). The organic phase was dried over Na_2SO_4 and concentrated in vacuo. The residue was purified by column chromatography (PE 40−60 °C/AcOEt 9:1 → 2:1) to afford **19a** as a colorless viscous oil (341 mg, 56%). ^{1}H NMR (200 MHz, $CDCl_3$) δ 1.29 (t, J = 7.1 Hz, 3H), 3.78 (s, 2H), 4.22 (q, J = 7.1 Hz, 2H), 5.59 (t, J = 1.3 Hz, 1H), 6.31 (s, 1H), 7.30−7.54 (m, 8H), 7.60−7.7 (m, 5H); ^{13}C NMR (50 MHz, $CDCl_3$) δ 14.3, 38.3, 61.0, 124.4, 126.5, 127.1, 127.4, 127.5, 128.9, 139.9, 140.3, 141.2, 142.0, 167.0. ES-MS m/z: calcd for $[C_{24}H_{22}O_2 + NH_4]^+$ 360.2; found, 360.2. HRMS (m/z): $[M + Na]^+$ calcd for $C_{24}H_{22}NaO_2^+$, 365.1512; found, 365.1516.

Ethyl 2-[(3,3″-Dichloro-[1,1′:3′,1″-terphenyl]-5′-yl)methyl]-acrylate (19b). Compound **18b** (741 mg, 1.89 mmol) was converted to **19b** by following the same procedure as described for the synthesis of **19a**. Colorless viscous oil (194 mg, 25%). ^{1}H NMR (200 MHz, $CDCl_3$) δ 1.27 (t, J = 7.1 Hz, 3H), 3.76 (s, 2H), 4.21 (q, J = 7.1 Hz, 2H), 5.59 (q, J = 1.2 Hz, 1H), 6.30 (br s, 1H), 7.18−7.67 (m, 11H); ^{13}C NMR (50 MHz, $CDCl_3$) δ 14.3, 38.3, 61.1, 124.3, 125.6, 126.7, 127.5, 127.7, 130.2, 134.8, 140.1, 140.4, 140.8, 142.8, 166.9. ES-MS m/z: calcd for $[C_{24}H_{20}Cl_2O_2 + NH_4]^+$ 428.1; found, 428.2. HRMS (m/z): $[M + Na]^+$ calcd for $C_{24}H_{20}Cl_2NaO_2^+$, 433.0733; found, 433.0737.

3′-(Adamantan-1-yl)-2′-{[((1*R*)-1-{[(*tert*-butoxy)carbonyl]-amino}-3-phenylpropyl)(hydroxy)phosphoryl]methyl}-propanoic Acid (21a). Addition of phosphinic acid 7 (300 mg, 1.00 mmol) to ethyl 2-[(adamant-1-yl)methyl]acrylate[28] (320 mg, 1.30 mmol) according to general procedure A and subsequent saponification according to general procedure B afforded compound **21a** as a mixture of two diastereoisomers (410 mg, 79% starting from **11**). ^{1}H NMR (200 MHz, DMSO-d_6) δ 1.19−2.09 (m, 30H), 2.30−2.54 and 2.55−2.82 (m, 3H), 3.32−3.67 (m, 1H), 6.90−7.35 (m, 5H); ^{13}C NMR (50 MHz, DMSO-d_6) δ 28.1, 28.3, 29.2, 29.8, 29.9, 32.5 (d, $^1J_{PC}$ = 77 Hz), 32.5, 32.7 (d, $^1J_{PC}$ = 80 Hz), 36.6, 41.8, 47.0, 47.6, 49.3 (d, $^1J_{PC}$ = 105 Hz), 49.7 (d, $^1J_{PC}$ = 105 Hz), 78.2, 78.6, 125.9, 128.4, 128.5, 141.4, 141.5, 155.7, 155.8, 177.4, 177.5, 177.6, 177.7; ^{31}P NMR (81 MHz, DMSO-d_6) δ 46.5. ES-MS m/z: calcd for $[C_{28}H_{42}NO_6P - H]^-$ 518.3; found, 518.4. HRMS (m/z): $[M + Na]^+$ calcd for $C_{28}H_{42}NNaO_6P^+$, 542.2642; found, 542.2645.

2′-{[((1*R*)-1-{[(*tert*-Butoxy)carbonyl]amino}-3-phenylpropyl)-(hydroxy)phosphoryl]methyl}-4′,4′-diphenylbutanoic Acid (21b). Addition of phosphinic acid 7 (300 mg, 1.00 mmol) to acrylic derivative **15** (308 mg, 1.10 mmol) according to general procedure A and subsequent saponification according to general procedure B afforded compound **21b** as a mixture of two diastereoisomers (336 mg, 61% starting from **11**). ^{1}H NMR (200 MHz, DMSO-d_6) δ 1.40 + 1.43 (2 × s, 9H), 1.63−2.06 (m, 4H), 2.07−2.28 (m, 1H), 2.35−2.81 (m, 4H), 3.41−3.70 (m, 1H), 3.89−4.08 (m, 1H), 6.66 (d, J = 9.3 Hz, 1H), 6.97−7.42 (m, 15H); ^{13}C NMR (50 MHz, DMSO-d_6) δ 27.9, 28.0, 28.3, 29.2, 29.3, 29.6, 29.7, 31.8, 32.0, 37.2, 48.6, 49.5 (d, $^1J_{PC}$ = 105 Hz), 49.8 (d, $^1J_{PC}$ = 106 Hz), 78.3, 78.4, 125.9, 126.2, 127.5, 128.0, 128.4, 128.6, 141.4, 143.6, 145.3, 155.7, 155.8, 176.0, 176.1, 176.2; ^{31}P NMR (81 MHz, DMSO-d_6) δ 46.5. ES-MS m/z: calcd for $[C_{31}H_{38}NO_6P - H]^-$ 550.2; found, 550.3. HRMS (m/z): $[M + H]^+$ calcd for $C_{31}H_{39}NO_6P^+$, 552.2510; found, 552.2515.

3′-([1,1′:3′,1″-Terphenyl]-5′-yl)-2′-{[((1*R*)-1-{[(*tert*-butoxy)-carbonyl]amino}-3-phenylpropyl)(hydroxy)phosphoryl]-methyl}propanoic Acid (21c). Addition of phosphinic acid 7 (200 mg, 0.67 mmol) to acrylic derivative **19a** (277 mg, 0.81 mmol) according to general procedure A and subsequent saponification according to general procedure B afforded compound **8** as a mixture of two diastereoisomers (362 mg, 88% starting from 7). ^{1}H NMR (200 MHz, DMSO-d_6) δ 1.34 + 1.41 (2 × s, 9H), 1.58−2.08 (m, 4H), 2.37−2.58 (m, 1H), 2.58−2.80 (m, 1H), 2.92−3.20 (m, 3H), 3.47−3.73 (m, 1H), 7.06−7.83 (m, 19H); ^{13}C NMR (50 MHz, DMSO-d_6) δ 26.4, 27.9, 28.2, 29.0, 29.2, 31.6, 31.9, 49.1 ($^1J_{PC}$ = 107 Hz), 49.5 ($^1J_{PC}$ = 107 Hz), 78.3, 78.4, 123.5, 125.9, 126.9, 127.1, 127.7, 128.4, 128.6, 128.8, 129.0, 140.1, 140.3, 141.0, 141.4, 141.5, 155.7, 155.8, 175.2, 175.4, 175.5, 175.6; ^{31}P NMR (81 MHz, DMSO-d_6) δ 46.7, 47.0. ES-MS m/z: calcd for $[C_{36}H_{40}NO_6P - H]^-$ 612.3; found, 612.4. HRMS (m/z): $[M + H]^+$ calcd for $C_{36}H_{41}NO_6P^+$, 614.2666; found, 614.2666.

3′-[((1*R*)-1-{[(*tert*-Butoxy)carbonyl]amino}-3-phenylpropyl)-(hydroxy)phosphoryl]-2′-[(3,3″-dichloro[1,1′:3′,1″-terphenyl]-5′-yl)methyl]propanoic Acid (21d). Addition of phosphinic acid 7 (175 mg, 0.58 mmol) to acrylic derivative **19b** (292 mg, 0.71 mmol) according to general procedure A and subsequent saponification according to general procedure B afforded compound **21d** as a mixture of two diastereoisomers (344 mg, 87% starting from 7). ^{1}H NMR (200 MHz, DMSO-d_6) δ 1.33 + 1.41 (2 × s, 9H), 1.59−2.08 (m, 4H), 2.31−2.51 (m, 1H), 2.58−2.80 (m, 1H), 2.92−3.16 (m, 3H), 3.44−3.71 (m, 1H), 7.03−7.93 (m, 17H); ^{13}C NMR (50 MHz, DMSO-d_6) δ 26.5, 27.9, 28.2, 28.9, 29.1, 31.6, 31.8, 49.4 ($^1J_{PC}$ = 106 Hz), 78.2, 78.3, 123.8, 125.8, 126.8, 127.5, 128.3, 128.5, 130.7, 133.8, 139.4, 140.4, 141.4, 142.2, 155.7, 175.3, 175.5; ^{31}P NMR (81 MHz, DMSO-d_6) δ 46.9, 47.1. ES-MS m/z: calcd for $[C_{36}H_{38}Cl_2NO_6P - H]^-$ 680.2; found, 680.3. HRMS (m/z): $[M + Na]^+$ calcd for $C_{36}H_{38}Cl_2NNaO_6P^+$, 704.1706; found, 704.1694.

((1*R*)-1-Amino-3-phenylpropyl){2′-[(adamantan-1-yl)-methyl]-3′-[((2″*S*)-1″-amino-1″-oxo-3″-phenylpropan-2″-yl)-amino]-3′-oxopropyl}phosphinic Acid (22a). Coupling of **21a** with HBr·H-(L)Phe-NH_2 (**5c**) according to general procedure D and subsequent deprotection according to general procedure C afforded compound **22a** as a mixture of two diastereoisomers (yield for two steps: 79%) which separated by semipreparative HPLC and tested separately. ^{1}H NMR (200 MHz, DMSO-d_6) δ 1.14−1.70 (m, 16H), 1.71−2.26 (m, 5H), 2.60−2.98 (m, 4H), 3.00−3.36 (m, 2H), 4.34−4.56 (m, 1H), 6.97−8.01 (m, 13H), 7.34−8.01 (m, 3H); ^{13}C NMR (50 MHz, DMSO-d_6/2% TFA) δ 28.3, 30.0, 30.1, 31.7, 31.9, 32.6, 32.7, 33.9, 34.9, 36.7, 37.1, 37.6, 41.7, 41.9, 47.5, 47.6, 48.5, 48.8, 48.8 (d, $^1J_{PC}$ = 94 Hz), 49.0 (d, $^1J_{PC}$ = 95 Hz), 54.4, 126.4, 128.3, 128.6, 128.8, 129.3, 129.5, 138.5, 138.9, 141.1, 141.2, 143.1, 173.4, 174.3, 175.0, 175.2, 175.5, 175.6; ^{31}P NMR (81 MHz, DMSO-d_6/2% TFA) δ 45.8, 45.9. HRMS (m/z): $[M - H]^-$ calcd for $C_{32}H_{43}N_3O_4P^-$, 564.2997; found, 564.2996.

((1*R*)-1-Amino-3-phenylpropyl){2′-[((2″*S*)-1″-amino-1″-oxo-3″-phenylpropan-2″-yl)carbamoyl]-4′,4′-diphenylbutyl}-phosphinic Acid (22b). Coupling of **21b** with HBr·H-(L)Phe-NH_2 (**5c**) according to general procedure D and subsequent deprotection according to general procedure C afforded compound **22b** as as a mixture of two diastereoisomers (yield for two steps: 80%) which were separated by semipreparative HPLC and tested separately. ^{1}H NMR (200 MHz, DMSO-d_6/2% TFA) δ 1.71−2.20 (m, 4H), 2.26−2.97 (m, 6H), 3.00−3.40 (m, 2H), 3.48−3.66 and 3.75−3.92 (m, 1H), 4.37−4.63 (m, 1H), 6.89−7.45 (m, 20H), 7.54−8.45 (m, 6H); ^{13}C NMR (50 MHz, DMSO-d_6/2% TFA) δ 29.7, 31.6, 31.8, 36.9, 37.1, 37.1, 37.8, 47.6, 47.6, 47.7, 47.9, 49.6, 49.8, 54.0, 126.3, 127.6, 127.6, 127.8, 128.1, 128.2, 128.5, 128.5, 128.7, 129.3, 138.4, 138.9, 140.9, 141.0, 144.2, 144.4, 144.6, 145.2, 173.3, 173.4, 173.6, 173.9, 174.1, 174.1; ^{31}P NMR (81 MHz, DMSO-d_6/2% TFA) δ 41.0. HRMS (m/z): $[M + H]^+$ calcd for $C_{35}H_{41}N_3O_4P^+$, 598.2829; found, 598.2830.

((1*R*)-1-Amino-3-phenylpropyl){2′-[((2″*S*)-1″-amino-4″-methyl-1″-oxopentan-2″-yl)carbamoyl]-4′,4′-diphenylbutyl}-phosphinic Acid (26c). Coupling of **21b** with HBr·H-(L)Leu-NH_2 (**5b**) according to general procedure D and subsequent deprotection according to general procedure C afforded compound **22d** as a white solid (yield for two steps: 75%). Due to the efficient chromatographic separation of diastereoisomers before the deprotection step, the isolation of the desired *RSS* (first eluted) isomer became feasible. ^{1}H NMR (500 MHz, DMSO-d_6/3% TFA) δ 0.84 (t, J = 5.9 Hz, 6H), 1.41−1.53 (m, 2H), 1.54−1.65 (m, 1H), 1.76−1.88 (m, 1H), 1.91−2.10 (m, 3H), 2.11−2.27 (m, 2H), 2.44−2.67 (m, 2H), 2.79 (dt, J = 4.7, 13.0 Hz, 1H), 3.16−3.27 (m, 1H), 3.95 (dd, J = 4.7, 10.0 Hz, 1H), 4.26 (dd, J = 8.0, 15.1 Hz, 1H), 7.01−7.55 (m, 17H), 7.80 (d, J = 7.9 Hz, 1H), 8.24 (br s, 3H); ^{13}C NMR (125 MHz, DMSO-d_6/3% TFA) δ 21.6, 23.1, 24.3, 29.6, 30.3, 31.6, 31.6, 38.5, 38.5, 40.6, 48.0, 48.6 ($^1J_{PC}$ = 94.5 Hz), 51.2, 126.1 126.2, 127.4, 128.0, 128.3, 128.5, 128.5,

DOI: 10.1021/acs.jmedchem.6b01031
J. Med. Chem. XXXX, XXX, XXX−XXX

128.6, 140.8, 145.0, 146.5, 173.4, 173.4, 174.3; ^{31}P NMR (81 MHz, DMSO-d_6/3% TFA) δ 41.4. HRMS (m/z): [M − H]$^-$ calcd for $C_{32}H_{41}N_3O_4P^-$, 562.2840; found, 562.2840.

((1*R*)-1-Amino-3-phenylpropyl){2′-([1,1′:3′,1″-terphenyl]-5′-ylmethyl)-3′-[((2″*S*)-1″-amino-1″-oxo-3″-phenylpropan-2″-yl)amino]-3′-oxopropyl}phosphinic Acid (22d). Coupling of **21c** with HBr·H-(L)Phe-NH_2 (**5c**) according to general procedure D and subsequent deprotection according to general procedure C afforded compound **22d** as a mixture of two diastereoisomers (yield for two steps: 78%), separated by semipreparative HPLC and tested separately. ^{1}H NMR (200 MHz, DMSO-d_6/3% TFA) δ 1.56−2.11 (m, 4H), 2.28−2.89 (m, 4H), 2.93−3.50 (m, 4H), 4.28−4.57 (m, 1H), 6.91−7.89 (m, 25H), 8.22 (br s, 3H), 8.40 (d, J = 8.9 Hz, 1H); ^{13}C NMR (50 MHz, DMSO-d_6) δ 27.1 ($^1J_{PC}$ = 92 Hz), 29.7, 31.6, 31.7, 37.7, 41.2, 48.6 ($^1J_{PC}$ = 95 Hz), 54.2, 123.6, 126.3, 127.0, 127.2, 127.7, 128.2, 128.3, 128.4, 128.6, 129.0, 129.4, 138.2, 140.3, 140.4, 140.9, 141.1, 172.9, 173.4, 173.5; ^{31}P NMR (81 MHz, DMSO-d_6/3% TFA) δ 41.3, 41.9. HRMS (m/z): [M − H]$^-$ calcd for $C_{40}H_{41}N_3O_4P^-$, 658.2840; found, 658.2846.

((1*R*)-1-Amino-3-phenylpropyl){2′-([1,1′:3′,1″-terphenyl]-5′-ylmethyl)-3′-[((2″*S*)-1″-amino-4″-methyl-1″-oxopentan-2″-yl)amino]-3′-oxopropyl}phosphinic Acid (22e). Coupling of **21c** with HBr·H-(L)Leu-NH_2 (**5b**) according to general procedure D and subsequent deprotection according to general procedure C afforded compound **22e** as a white solid (yield for two steps: 65%). Due to the efficient chromatographic separation of diastereoisomers before the deprotection step, the isolation of the desired *RSS* (first eluted) isomer became feasible. ^{1}H NMR (500 MHz, DMSO-d_6/3% TFA) δ 0.80 (dd, J = 6.4, 21.2 Hz, 6H), 1.39−1.61 (m, 3H), 1.71−1.87 (m, 2H), 1.93−2.05 (m, 1H), 2.29 (dt, J = 9.9, 15.2 Hz, 1H), 2.53−2.62 (m, 1H), 2.76 (dt, J = 4.8, 12.9 Hz, 1H), 2.91 (dt, J = 7.7, 13.0 Hz, 1H), 3.09−3.29 (m, 3H), 4.22 (dd, J = 8.7, 14.4 Hz, 1H), 6.84−7.91 (m, 20H), 8.25 (br s, 3H), 8.30 (d, J = 8.3 Hz, 1H); ^{13}C NMR (50 MHz, DMSO-d_6/3% TFA) 21.6, 23.2, 24.2, 28.2 ($^1J_{PC}$ = 94.4 Hz), 29.6, 31.6, 31.7, 41.0, 48.6 ($^1J_{PC}$ = 90.5 Hz), 51.2, 124.1, 126.2, 127.0, 127.1, 127.6, 128.2, 128.5, 128.9, 140.1, 140.3, 140.8, 141.0, 173.3, 173.4, 174.2; ^{31}P NMR (81 MHz, DMSO-d_6/3% TFA) δ 41.9. HRMS (m/z): [M − H]$^-$ calcd for $C_{37}H_{43}N_3O_4P^-$, 624.2997; found, 624.2999.

((1*R*)-1-Amino-3-phenylpropyl){3′-[((2″*S*)-1″-amino-4″-methyl-1″-oxopentan-2″-yl)amino]-2′-[(3,3″-dichloro-[1,1′:3′,1″-terphenyl]-5′-yl)methyl]-3′-oxopropyl}phosphinic Acid (22f). Coupling of **21d** with HBr·H-(L)Leu-NH_2 (**5b**) according to general procedure D and subsequent deprotection according to general procedure C afforded compound **22f** as a white solid (yield for two steps: 40%). Due to the efficient chromatographic separation of diastereoisomers before the deprotection step, the isolation of the desired *RSS* (first eluted) isomer became feasible. ^{1}H NMR (200 MHz, DMSO-d_6/2% TFA) δ 0.63−0.98 (m, 6H), 1.35−1.64 (m, 3H), 1.65−2.09 (m, 3H), 2.18−2.40 (m, 1H), 2.50−3.37 (m, 6H), 4.06−4.32 (m, 1H), 6.84−7.91 (m, 19H), 8.29 (br s, 3H); ^{13}C NMR (50 MHz, DMSO-d_6/2% TFA) 21.6, 23.3, 24.4, 28.3 ($^1J_{PC}$ = 91.4 Hz), 29.8, 31.7, 31.9, 41.1, 41.2, 48.8 ($^1J_{PC}$ = 95.4 Hz), 51.4, 126.1, 126.4, 127.0, 127.7, 127.8, 128.4, 128.7, 139.7, 140.6, 140.9, 142.4, 173.4, 173.5, 174.5; ^{31}P NMR (81 MHz, DMSO-d_6/2% TFA) δ 41.9. HRMS (m/z): [M − H]$^-$ calcd for $C_{37}H_{41}Cl_2N_3O_4P^-$, 692.2217; found, 692.2228.

Protein Expression and Purification. ERAP1 and ERAP2 were expressed by insect cell culture (Hi5) after infection with recombinant baculovirus as described.[5b,6c] IRAP was expressed by HEK 293S GnTI$^{(-)}$ as previously described.[5c]

In Vitro Enzymatic Assays. Evaluation of the inhibitory potency of the compounds was carried out using an in vitro fluorimetric assay as previously described.[35]

Cross-Presentation Assay. Spleens from C57Bl/6 wild-type (Janvier Labs, France) and from IRAP$^{-/-}$ mice bred in the animal facility of INSERM U1151 were digested with Liberase 500 μg/mL and DNase-1 10 ng/mL (Roche Laboratories) for 30 min at 37 °C in PBS. Enzymatic digestion was terminated by incubating cells on ice and adding IMDM medium supplemented with 10% FBS. After washing, CD11c+ cells were positively selected using paramagnetic beads (Miltenyi Biotec), following the manufacturer's protocol. The cells were then incubated with anti-CD11c/Brilliant Violet 421 (clone N418, Sony Biotechnology), anti-CD8α/Brilliant Violet 605 (clone 53-6.7, BD Biosciences), and anti-CD11b/PE-Cy7 (clone M1/70, BD Biosciences) for 30 min on ice. After washes and addition of 7-actinomycin D (7-AAD), the two main subsets of conventional dendritic cells (cDCs) were sorted using a BD FACS ARIA-II cell sorter as 7-AAD-CD11c+CD11b^{low}CD8α+ cells for CD8α+ cDCs, and 7-AAD-CD11c+CD11b^{high}CD8α- cells for CD11b+ cDCs. 15 000 sorted and washed cDCs resuspended in IMDM medium supplemented with penicillin, streptomycin, and 10% FBS were added per well in a 96-well plate with round bottom. Serial dilutions from 3 to 3333 nM of the inhibitor **22b** or DMSO was added to the cells for 60 min before the addition of 500 ng/mL of soluble ovalbumin in the presence of the same concentration of **22b** or DMSO. After 6 h, cells were washed in PBS and fixed with 50 μL of a PBS-glutaraldehyde 0.008% solution for 30 s to stop antigen processing and washed again twice with a solution containing PBS-glycine 0.2 M and once with PBS. As a negative control, some of the cells were fixed before the addition of **22b**. Finally, 45 000 TCR-transgenic CD8+ T cells per well, prepared from lymph nodes of Rag-1$^{-/-}$ C57Bl/6 OT-I mice, were added to the fixed cells and supernatants were collected after 24 h. OT-I T cell activation was assessed by dosing IL-2 concentration in supernatants using a sandwich ELISA assay: anti-IL2 (clone JES6-1A12, BD Biosciences) was used as a capture antibody, and anti-IL-2-biotin (clone JES6-5H4, BD Biosciences), streptavidin/horseradish peroxidase (HRP, Pierce), and tetramethylbenzidine substrate (BD Biosciences) were used for the detection of captured IL-2. Optical density was measured on a Mithras plate reader. Background (optical density from wells that contained prefixed cells) was subtracted from all specific values. All conditions were tested in triplicate.

Computational Methods. Docking calculations were performed as described previously,[35] using the crystallographic structures of ERAP1 (PDB code 2YD0), ERAP2 (PDB code 3SE6), and IRAP (PDB code 4PJ6) without further refinement.

■ ASSOCIATED CONTENT

Supporting Information

The Supporting Information is available free of charge on the ACS Publications website at DOI: 10.1021/acs.jmedchem.6b01031.

Experimental procedures and characterization for compounds **1**, **5b**, **5c**, **5f−j**, **11h**, and **11i**; list of RP-HPLC retention times and MS data for all tested compounds; titration of T-cell responses versus BMDCs exposed to different amounts of soluble ovalbumin (PDF)

Molecular formula strings and some data (CSV)

■ AUTHOR INFORMATION

Corresponding Authors

*E.S.: e-mail, stratos@rrp.demokritos.gr; phone, (+30) 2106503918; fax, (+30)2106503918.

*D.G.: e-mail, dgeorgia@chem.uoa.gr; phone, (+30) 2107274903; fax, (+30)2107274761.

Author Contributions

P.K. designed the synthetic routes and performed the synthesis and characterization of reported inhibitors with the contributions of I.D., I.P., S.K., M.P., S.A., and T.-M.F.; A.M. prepared the recombinant enzymes and performed the HPLC purification and in vitro assays. F.-X.M. and P.v.E. designed and performed the cross-presentation assay. A.P. contributed to SAR by performing molecular modeling analysis. D.G. and E.S. conceived the experiments, designed the inhibitors, analyzed the results, and supervised the project. All authors contributed

DOI: 10.1021/acs.jmedchem.6b01031
J. Med. Chem. XXXX, XXX, XXX−XXX

to the preparation of the manuscript and have approved its final version.

Notes

The authors declare no competing financial interest.

■ ACKNOWLEDGMENTS

This research was financed by the Special Account for Research Grants of National and Kapodistrian University of Athens and by the European Union (European Social Fund) and Greek national funds through the Operational Program "Education and Lifelong Learning" of the National Strategic Reference Framework: Research Funding Program of the General Secretariat for Research and Technology (Grant ERC-14 to E.S.). Funding was also provided by an award from the Harry J. Lloyd Charitable trust to E.S. Work in the laboratory of P.v.E. was supported by Grant DEQ20130326539 from the Fondation pour la Recherche Medicale and Grant ANR-14-CE11-0014 from the Agence Nationale de Recherche. D.G. thanks Dr. Vincent Dive and Dr. Laurent Devel for their kind support and valuable discussions and Dr. Maroula Kokotou for HRMS measurements.

■ ABBREVIATIONS USED

CCR2, CC chemokine receptor 2; CCL2, CC chemokine ligand 2; CCR5, CC chemokine receptor 5; DCC, *N,N′*-dicyclohexylcarbodiimide; DIPEA, *N,N*-diisopropylethylamine; DMAP, 4-dimethylaminopyridine; DMF, *N,N*-dimethylformamide; EDC·HCl, *N*-(3-dimethylaminopropyl)-*N′*-ethylcarbodiimide hydrochloride; HMDS, 1,1,1,3,3,3-hexamethyldisilazane; HOBt, 1-hydroxybenzotriazole; MMP, matrix metalloproteinase; TBS, *tert*-butyldimethylsilyl; TFA, trifluoroacetic acid; TIS, triisopropylsilane; TLC, thin layer chromatography

■ REFERENCES

(1) Evnouchidou, I.; Papakyriakou, A.; Stratikos, E. A new role for Zn(II) aminopeptidases: antigenic peptide generation and destruction. *Curr. Pharm. Des.* **2009**, *15*, 3656−3670.

(2) Weimershaus, M.; Evnouchidou, I.; Saveanu, L.; van Endert, P. Peptidases trimming MHC class I ligands. *Curr. Opin. Immunol.* **2013**, *25*, 90−96.

(3) Tsujimoto, M.; Hattori, A. The oxytocinase subfamily of M1 aminopeptidases. *Biochim. Biophys. Acta, Proteins Proteomics* **2005**, *1751*, 9−18.

(4) (a) Saveanu, L.; Carroll, O.; Weimershaus, M.; Guermonprez, P.; Firat, E.; Lindo, V.; Greer, F.; Davoust, J.; Kratzer, R.; Keller, S. R.; Niedermann, G.; van Endert, P. IRAP identifies an endosomal compartment required for MHC class I cross-presentation. *Science* **2009**, *325*, 213−217. (b) Segura, E.; Albiston, A. L.; Wicks, I. P.; Chai, S. Y.; Villadangos, J. A. Different cross-presentation pathways in steady-state and inflammatory dendritic cells. *Proc. Natl. Acad. Sci. U. S. A.* **2009**, *106*, 20377−20381.

(5) (a) Zervoudi, E.; Papakyriakou, A.; Georgiadou, D.; Evnouchidou, I.; Gajda, A.; Poreba, M.; Salvesen, G. S.; Drag, M.; Hattori, A.; Swevers, L.; Vourloumis, D.; Stratikos, E. Probing the S1 specificity pocket of the aminopeptidases that generate antigenic peptides. *Biochem. J.* **2011**, *435*, 411−420. (b) Mpakali, A.; Giastas, P.; Mathioudakis, N.; Mavridis, I. M.; Saridakis, E.; Stratikos, E. Structural basis for antigenic peptide recognition and processing by ER aminopeptidase 2. *J. Biol. Chem.* **2015**, *290*, 26021−26032. (c) Mpakali, A.; Saridakis, E.; Harlos, K.; Zhao, Y.; Papakyriakou, A.; Kokkala, P.; Georgiadis, D.; Stratikos, E. Crystal structure of insulin-regulated aminopeptidase with bound substrate analogue provides insight on antigenic epitope precursor recognition and processing. *J. Immunol.* **2015**, *195*, 2842−2851.

(6) (a) Birtley, J. R.; Saridakis, E.; Stratikos, E.; Mavridis, I. M. The crystal structure of human endoplasmic reticulum aminopeptidase 2 reveals the atomic basis for distinct roles in antigen processing. *Biochemistry* **2012**, *51*, 286−295. (b) Stratikos, E.; Stern, L. J. Antigenic peptide trimming by ER aminopeptidases—Insights from structural studies. *Mol. Immunol.* **2013**, *55*, 212−219. (c) Stamogiannos, A.; Koumantou, D.; Papakyriakou, A.; Stratikos, E. Effects of polymorphic variation on the mechanism of Endoplasmic Reticulum Aminopeptidase 1. *Mol. Immunol.* **2015**, *67*, 426−435.

(7) (a) Cagliani, R.; Riva, S.; Biasin, M.; Fumagalli, M.; Pozzoli, U.; Lo Caputo, S.; Mazzotta, F.; Piacentini, L.; Bresolin, N.; Clerici, M.; Sironi, M. Genetic diversity at endoplasmic reticulum aminopeptidases is maintained by balancing selection and is associated with natural resistance to HIV-1 infection. *Hum. Mol. Genet.* **2010**, *19*, 4705−4714. (b) Fierabracci, A.; Milillo, A.; Locatelli, F.; Fruci, D. The putative role of endoplasmic reticulum aminopeptidases in autoimmunity: insights from genomic-wide association studies. *Autoimmun. Rev.* **2012**, *12*, 281−288. (c) Seregin, S. S.; Rastall, D. P. W.; Evnouchidou, I.; Aylsworth, C. F.; Quiroga, D.; Kamal, R. P.; Godbehere-Roosa, S.; Blum, C. F.; York, I. A.; Stratikos, E.; Amalfitano, A. Endoplasmic reticulum aminopeptidase-1 alleles associated with increased risk of ankylosing spondylitis reduce HLA-B27 mediated presentation of multiple antigens. *Autoimmunity* **2013**, *46*, 497−508. (d) Stratikos, E.; Stamogiannos, A.; Zervoudi, E.; Fruci, D. A role for naturally occurring alleles of endoplasmic reticulum aminopeptidases in tumor immunity and cancer pre-disposition. *Front. Oncol.* **2014**, *4*, 363.

(8) Fruci, D.; Romania, P.; D'Alicandro, V.; Locatelli, F. Endoplasmic reticulum aminopeptidase 1 function and its pathogenic role in regulating innate and adaptive immunity in cancer and major histocompatibility complex class I-associated autoimmune diseases. *Tissue Antigens* **2014**, *84*, 177−186.

(9) Goto, Y.; Ogawa, K.; Nakamura, T. J.; Hattori, A.; Tsujimoto, M. TLR-mediated secretion of endoplasmic reticulum aminopeptidase 1 from macrophages. *J. Immunol.* **2014**, *192*, 4443−4452.

(10) (a) Stratikos, E. Modulating antigen processing for cancer immunotherapy. *Oncoimmunology* **2014**, *3*, e27568. (b) Stratikos, E. Regulating adaptive immune responses using small molecule modulators of aminopeptidases that process antigenic peptides. *Curr. Opin. Chem. Biol.* **2014**, *23*, 1−7.

(11) Zervoudi, E.; Saridakis, E.; Birtley, J. R.; Seregin, S. S.; Reeves, E.; Kokkala, P.; Aldhamen, Y. A.; Amalfitano, A.; Mavridis, I. M.; James, E.; Georgiadis, D.; Stratikos, E. Rationally designed inhibitor targeting antigen-trimming aminopeptidases enhances antigen presentation and cytotoxic T-cell responses. *Proc. Natl. Acad. Sci. U. S. A.* **2013**, *110*, 19890−19895.

(12) (a) Aldhamen, Y. A.; Pepelyayeva, Y.; Rastall, D. P. W.; Seregin, S. S.; Zervoudi, E.; Koumantou, D.; Aylsworth, C. F.; Quiroga, D.; Godbehere, S.; Georgiadis, D.; Stratikos, E.; Amalfitano, A. Autoimmune disease-associated variants of extracellular endoplasmic reticulum aminopeptidase 1 induce altered innate immune responses by human immune cells. *J. Innate Immun.* **2015**, *7*, 275−289. (b) Chen, L.; Ridley, A.; Hammitzsch, A.; Al-Mossawi, M. H.; Bunting, H.; Georgiadis, D.; Chan, A.; Kollnberger, S.; Bowness, P. Silencing or inhibition of endoplasmic reticulum aminopeptidase 1 (ERAP1) suppresses free heavy chain expression and Th17 responses in ankylosing spondylitis. *Ann. Rheum. Dis.* **2016**, *75*, 916−923.

(13) (a) Dive, V.; Cotton, J.; Yiotakis, A.; Michaud, A.; Vassiliou, S.; Jiracek, J.; Vazeux, G.; Chauvet, M. T.; Cuniasse, P.; Corvol, P. RXP 407, a phosphinic peptide, is a potent inhibitor of angiotensin I converting enzyme able to differentiate between its two active sites. *Proc. Natl. Acad. Sci. U. S. A.* **1999**, *96*, 4330−4335. (b) Georgiadis, D.; Cuniasse, P.; Cotton, J.; Yiotakis, A.; Dive, V. Structural determinants of RXPA380, a potent and highly selective inhibitor of the angiotensin-converting enzyme C-domain. *Biochemistry* **2004**, *43*, 8048−8054.

(14) Devel, L.; Rogakos, V.; David, A.; Makaritis, A.; Beau, F.; Cuniasse, P.; Yiotakis, A.; Dive, V. Development of selective inhibitors and substrate of matrix metalloproteinase-12. *J. Biol. Chem.* **2006**, *281*, 11152−11160.

DOI: 10.1021/acs.jmedchem.6b01031
J. Med. Chem. XXXX, XXX, XXX−XXX

(15) Georgiadis, D.; Dive, V. Phosphinic peptides as potent inhibitors of zinc-metalloproteases. *Top. Curr. Chem.* **2014**, *360*, 1−38.
(16) Yiotakis, A.; Georgiadis, D.; Matziari, M.; Makaritis, A.; Dive, V. Phosphinic peptides: Synthetic approaches and biochemical evaluation as Zn-metalloprotease inhibitors. *Curr. Org. Chem.* **2004**, *8*, 1135−1158.
(17) (a) Jullien, N.; Makritis, A.; Georgiadis, D.; Beau, F.; Yiotakis, A.; Dive, V. Phosphinic tripeptides as dual angiotensin-converting enzyme C-domain and endothelin-converting enzyme-1 inhibitors. *J. Med. Chem.* **2010**, *53*, 208−220. (b) Masuyer, G.; Akif, M.; Czarny, B.; Beau, F.; Schwager, S. L. U.; Sturrock, E. D.; Isaac, R. E.; Dive, V.; Acharya, K. R. Crystal structures of highly specific phosphinic tripeptide enantiomers in complex with the angiotensin-I converting enzyme. *FEBS J.* **2014**, *281*, 943−956.
(18) Mucha, A.; Drag, M.; Dalton, J. P.; Kafarski, P. Metallo-aminopeptidase inhibitors. *Biochimie* **2010**, *92*, 1509−1529.
(19) (a) Chen, H.; Noble, F.; Mothé, A.; Meudal, H.; Coric, P.; Danascimento, S.; Roques, B. P.; George, P.; Fournié-Zaluski, M. C. Phosphinic derivatives as new dual enkephalin-degrading enzyme inhibitors: Synthesis, biological properties, and antinociceptive activities. *J. Med. Chem.* **2000**, *43*, 1398−1408. (b) Mucha, A.; Lämmerhofer, M.; Lindner, W.; Pawełczak, M.; Kafarski, P. Individual stereoisomers of phosphinic dipeptide inhibitor of leucine amino-peptidase. *Bioorg. Med. Chem. Lett.* **2008**, *18*, 1550−1554.
(20) Makaritis, A.; Georgiadis, D.; Dive, V.; Yiotakis, A. Diastereoselective solution and multipin-based combinatorial array synthesis of a novel class of potent phosphinic metalloprotease inhibitors. *Chem. - Eur. J.* **2003**, *9*, 2079−2094.
(21) (a) David, A.; Steer, D.; Bregant, S.; Devel, L.; Makaritis, A.; Beau, F.; Yiotakis, A.; Dive, V. Cross-linking yield variation of a potent matrix metalloproteinase photoaffinity probe and consequences for functional proteomics. *Angew. Chem., Int. Ed.* **2007**, *46*, 3275−3277. (b) Mores, A.; Matziari, M.; Beau, F.; Cuniasse, P.; Yiotakis, A.; Dive, V. Development of potent and selective phosphinic peptide inhibitors of angiotensin-converting enzyme 2. *J. Med. Chem.* **2008**, *51*, 2216−2226. (c) Marchant, D. J.; Bellac, C. L.; Moraes, T. J.; Wadsworth, S. J.; Dufour, A.; Butler, G. S.; Bilawchuk, L. M.; Hendry, R. G.; Robertson, A. G.; Cheung, C. T.; Ng, J.; Ang, L.; Luo, Z.; Heilbron, K.; Norris, M. J.; Duan, W.; Bucyk, T.; Karpov, A.; Devel, L.; Georgiadis, D.; Hegele, R. G.; Luo, H.; Granville, D. J.; Dive, V.; McManus, B. M.; Overall, C. M. A new transcriptional role for matrix metalloproteinase-12 in antiviral immunity. *Nat. Med.* **2014**, *20*, 493−502.
(22) (a) Chen, H.; Noble, F.; Roques, B. P.; Fournié-Zaluski, M. C. Long lasting antinociceptive properties of enkephalin degrading enzyme (NEP and APN) inhibitor prodrugs. *J. Med. Chem.* **2001**, *44*, 3523−3530. (b) Matziari, M.; Dellis, D.; Dive, V.; Yiotakis, A.; Samios, J. Conformational and solvation studies via computer simulation of the novel large scale diastereoselectively synthesized phosphinic MMP inhibitor RXP03 diluted in selected solvents. *J. Phys. Chem. B* **2010**, *114*, 421−428.
(23) Lämmerhofer, M.; Hebenstreit, D.; Gavioli, E.; Lindner, W.; Mucha, A.; Kafarski, P.; Wieczorek, P. High-performance liquid chromatographic enantiomer separation and determination of absolute configurations of phosphinic acid analogues of dipeptides and their α-aminophosphinic acid precursors. *Tetrahedron: Asymmetry* **2003**, *14*, 2557−2565.
(24) Baylis, E. K.; Campbell, C. D.; Dingwall, J. G. 1-Amino-alkylphosphonous acids. Part 1. Isosteres of the protein amino acids. *J. Chem. Soc., Perkin Trans. 1* **1984**, 2845−2853.
(25) Kummer, D. A.; Chain, W. J.; Morales, M. R.; Quiroga, O.; Myers, A. G. Stereocontrolled alkylative construction of quaternary carbon centers. *J. Am. Chem. Soc.* **2008**, *130*, 13231−13233.
(26) Georgiadis, D.; Matziari, M.; Vassiliou, S.; Dive, V.; Yiotakis, A. A convenient method to synthesize phosphinic peptides containing an aspartyl or glutamyl aminophosphinic acid. Use of the phenyl group as the carboxyl synthon. *Tetrahedron* **1999**, *55*, 14635−14648.
(27) Christl, M.; Huisgen, R. 1,3-Dipolare Cycloadditionen, 74. Orientierungsphänomene bei cycloadditionen aliphatischer und aromatischer nitriloxide an α,β-ungesättigte carbonester. *Chem. Ber.* **1973**, *106*, 3345−3367.
(28) Baldwin, J. E.; Adlington, R. M.; Birch, D. J.; Crawford, J. A.; Sweeney, J. B. Radical reactions in synthesis: carbon-carbon bond formation from 2-substituted allyl trialkyl stannanes. *J. Chem. Soc., Chem. Commun.* **1986**, 1339−1340.
(29) Hin, B.; Majer, P.; Tsukamoto, T. Facile synthesis of α-substituted acrylate esters. *J. Org. Chem.* **2002**, *67*, 7365−7368.
(30) Hamilton, J. Y.; Sarlah, D.; Carreira, E. M. Iridium-catalyzed enantioselective allyl-alkene coupling. *J. Am. Chem. Soc.* **2014**, *136*, 3006−3009.
(31) Devel, L.; Garcia, S.; Czarny, B.; Beau, F.; LaJeunesse, E.; Vera, L.; Georgiadis, D.; Stura, E.; Dive, V. Insights from selective non-phosphinic inhibitors of MMP-12 tailored to fit with an S1′ loop canonical conformation. *J. Biol. Chem.* **2010**, *285*, 35900−35909.
(32) Nguyen, T. T.; Chang, S.-C.; Evnouchidou, I.; York, I. A.; Zikos, C.; Rock, K. L.; Goldberg, A. L.; Stratikos, E.; Stern, L. J. Structural basis for antigenic peptide precursor processing by the endoplasmic reticulum aminopeptidase ERAP1. *Nat. Struct. Mol. Biol.* **2011**, *18*, 604−613.
(33) (a) Andersson, H.; Demaegdt, H.; Vauquelin, G.; Lindeberg, G.; Karlén, A.; Hallberg, M.; Erdélyi, M.; Hallberg, A. Disulfide cyclized tripeptide analogues of angiotensin IV as potent and selective inhibitors of Insulin-Regulated Aminopeptidase (IRAP). *J. Med. Chem.* **2010**, *53*, 8059−8071. (b) Andersson, H.; Demaegdt, H.; Johnsson, A.; Vauquelin, G.; Lindeberg, G.; Hallberg, M.; Erdélyi, M.; Karlén, A.; Hallberg, A. Potent macrocyclic inhibitors of Insulin-Regulated Aminopeptidase (IRAP) by olefin ring-closing metathesis. *J. Med. Chem.* **2011**, *54*, 3779−3792.
(34) Bukhaltsev, E.; Goldberg, I.; Cohen, R.; Vigalok, A. Tunable π-interactions in monomeric organozinc complexes: solution and solid-state studies. *Organometallics* **2007**, *26*, 4015−4020.
(35) Papakyriakou, A.; Zervoudi, E.; Tsoukalidou, S.; Mauvais, F. X.; Sfyroera, G.; Mastellos, D. C.; van Endert, P.; Theodorakis, E. A.; Vourloumis, D.; Stratikos, E. 3,4-Diaminobenzoic acid derivatives as inhibitors of the oxytocinase subfamily of M1 aminopeptidases with immune-regulating properties. *J. Med. Chem.* **2015**, *58*, 1524−1543.
(36) Morrison, R. A.; Singhvi, S. M.; Peterson, A. E.; Pocetti, D. A.; Migdalof, B. H. Relative contribution of the gut, liver, and lung to the first-pass hydrolysis (bioactivation) of orally administered 14C-fosinopril sodium in dogs. In vivo and in vitro studies. *Drug Metab. Dispos.* **1990**, *18*, 253−257.
(37) Gottlieb, H. E.; Kotlyar, V.; Nudelman, A. NMR Chemical shifts of common laboratory solvents as trace impurities. *J. Org. Chem.* **1997**, *62*, 7512−7515.

DOI: 10.1021/acs.jmedchem.6b01031
J. Med. Chem. XXXX, XXX, XXX−XXX